IEEE Access
Multidisciplinary ⋮ Rapid Review ⋮ Open Access Journal

Received July 30, 2019, accepted August 3, 2019, date of publication August 6, 2019, date of current version August 21, 2019.

Digital Object Identifier 10.1109/ACCESS.2019.2933493

Excitation System Technologies for Wound-Field Synchronous Machines: Survey of Solutions and Evolving Trends

JONAS KRISTIANSEN NØLAND[1], (Member, IEEE), STEFANO NUZZO[2,3], (Member, IEEE), ALBERTO TESSAROLO[4], (Senior Member, IEEE), AND ERICK FERNANDO ALVES[1], (Senior Member, IEEE)

[1]Department of Electric Power Engineering, Norwegian University of Science and Technology (NTNU), 7034 Trondheim, Norway
[2]PEMC Group, University of Nottingham, Nottingham NG7 2RD, U.K.
[3]Department of Engineering Enzo Ferrari, University of Modena and Reggio Emilia, 41125 Modena, Italy
[4]Department of Engineering and Architecture, University of Trieste, Trieste, Italy

Corresponding author: Jonas Kristiansen Nøland (jonas.k.noland@ntnu.no)

This work was supported by the Open Access funding granted from the NTNU Publishing Fund.

ABSTRACT Wound-field synchronous machines (WFSMs) are included in the majority of large power generating units and special high-power motor drives, due to their high efficiency, flexible field excitation and intrinsic flux weakening capability. Moreover, they are employed in a wide range of high-end solutions in the low-to-medium power range. This contribution presents a comprehensive survey of classical and modern methods and technologies for excitation systems (ESs) of WFSMs. The work covers the fundamental theory, typical de-excitation methods and all the modern excitation equipment topologies in detail. It also includes a description of the state-of-the-art and the latest trends in the ESs of wound-field synchronous motors and generators. The purpose of the paper is to provide a useful and up-to-date reference for practitioners and researchers in the field.

INDEX TERMS Brushless exciters, de-excitation methods, excitation systems, exciterless excitation, harmonic excitation, rotating exciters, static exciters, synchronous machines, synchronous generators, synchronous motors.

I. INTRODUCTION

Wound-field synchronous machines (WFSMs) are the preferred choice in power generation applications ranging from few kVA to few GVA [1]. The main reasons are:

1) the possibility to control the flow of reactive power (both absorption and production);
2) the intrinsic flux regulation capability;
3) the reliability and resilience to short-circuit faults with no demagnetization risks;
4) the high efficiency;
5) and the superior dynamics during electro-mechanical transients.

WFSMs are predominant in grid-connected operations [2] and in small-to-medium generating systems for isolated applications [3], [4]. Moreover, wound-field synchronous motors are still today the preferred choice for high-power applications in the multi-MW range [5], [6], especially in the oil-and-gas industry [7]–[9] and for large shipboard propulsion [10]. Although these machines represent a consolidated and mature technology, much attention is currently given to their design [11], analysis [12], modelling [13], as well as to their field excitation technologies [14]. While most of the research on permanent magnet (PM) synchronous motor and generator performance enhancement relies on sophisticated control algorithms [15], [16], a key role in WFSM development is played by new hardware and design solutions for the improvement of rotor excitation in terms of dynamic performance [17], reliability [18], compactness [19]–[22] and condition monitoring [23]–[25].

The art of ESs for WFSMs is an old engineering discipline. Fig. 1 shows a high-level sketch of its development history. Its first dramatic change happened in the 1950s as a result of advances in high-power semiconductor devices. This triggered the replacement of electromechanical regulators, based on direct-current commutators [26], by

The associate editor coordinating the review of this manuscript and approving it for publication was Xiaodong Sun.

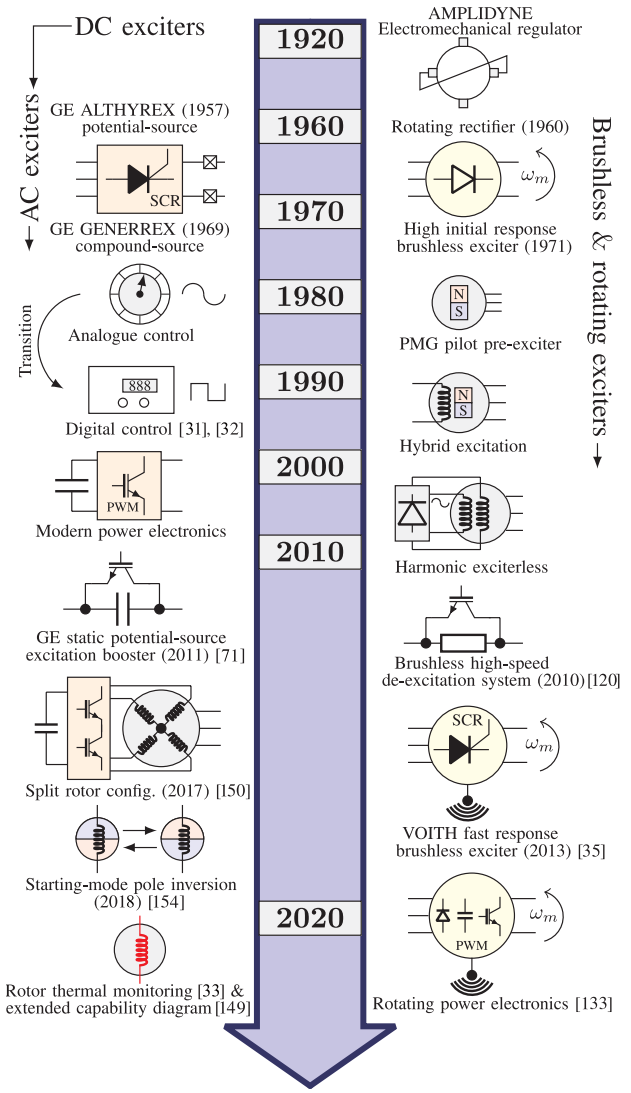

FIGURE 1. Development history of excitation systems for wound-field synchronous machines.

silicon-controlled rectifiers (SCRs) and analogue controllers [27], [28]. Another paradigm shift happened in the 1980s, when controllers migrated from analogue to digital technology [29]–[32].

Over the last 20 years, the evolution of power electronics and wireless technologies has enabled further innovations and possibilities in the area. Currently, the static excitation methods (in which the field winding is fed through brushes and shaft-mounted slip rings) are preferred whenever a fast dynamic response is required. However, they cause maintenance and safety issues due to brush wear and possible sparking. Brushless exciters (where power is supplied to the field winding by electromagnetic induction with no sliding contacts) overcome these challenges. On the other hand, they suffer from worse dynamic performance, prevent direct access to the field winding for measurement and protection purposes, and require the installation of an auxiliary rotating machine (exciter) on the main motor or generator shaft. Nevertheless, such limitations are being significantly reduced by the advances currently in progress. For example, integrated-harmonic brushless exciterless solutions are a promising trend for the most compact options on the market [19]–[22]. In addition, wireless communication can be nowadays used to measure field winding quantities [33], and employed to regulate the excitation current through shaft-installed, remote-controlled power electronics devices [34]–[41], thus overcoming some limitations of brushless exciters.

The main focus of this paper is to provide a comprehensive and general review of the different excitation architectures for WFSMs. The fundamental theory of field excitation, step responses and de-excitation is first recalled in Section II. Section III presents an extensive survey of the possible excitation technologies presently available or under development, pointing out their pros and cons. Finally, Section VI concludes the paper by summarizing the work and discussing the most promising perspectives for future development.

II. THE FUNDAMENTALS OF FIELD EXCITATION

An ES encompasses the equipment used to provide field current to a synchronous machine, including power regulation and control, as well as protective elements [42]–[48]. The ES fits the basic construction principle of a WFSMs, which include a set of rotating poles equipped with a field winding fed by direct current and a stationary armature winding which carry alternating currents. The operating principle of the WFSM is extensively described in the technical literature [49].

The field winding of the WFSM is subjected to the ES output, which is the field voltage. The latter is referred to as U_{f0} at no-load and U_f at rated conditions. The dynamics of an ES is strongly influenced by the field winding inductance, which can be regarded as a constant except for magnetic saturation effects. The relationship between the field winding inductance (L_f) and the field winding resistance (R_f) in open-circuit conditions is

$$L_f = T'_{do} R_f, \tag{1}$$

where T'_{do} is the d-axis transient open-circuit time constant of the generator, or the time constant of the rotor in no-load conditions. During steady-state operation, the field winding needs to be supplied with a (constant) rated voltage U_{f0} and a (constant) rated current I_{f0} satisfying the following equation

$$U_{f0} = R_f I_{f0}. \tag{2}$$

The dynamics of the field winding during no-load operation is governed by a first-order differential equation, i.e.

$$u_f = R_f i_f + L_f \frac{di_f}{dt}. \tag{3}$$

where u_f and i_f are the instantaneous field voltage and field current, respectively. The automatic voltage regulator (AVR)

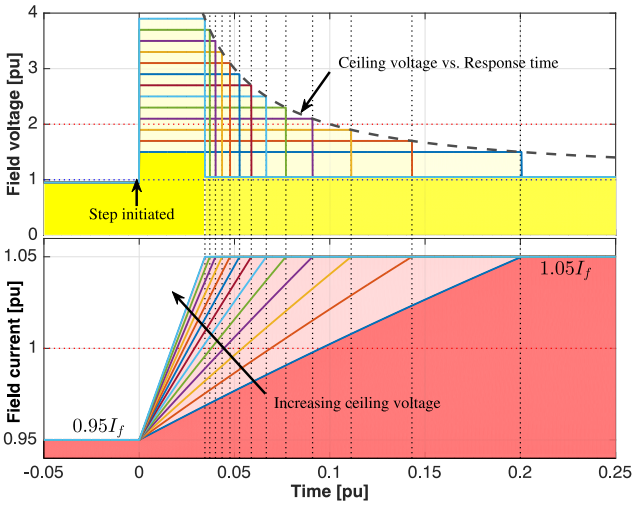

FIGURE 2. Illustration of an ideal field current step response from 0.95*pu* to 1.05*pu*, for several ceiling voltage values. The time is normalized with respect to T'_{do} for no-load conditions and to T'_d for on-load conditions (first approximation).

typically acts in the per-unit frame, where the field voltage is expressed as a fraction of the rated field voltage, i.e.:

$$u_f = \gamma_f U_{f0} \tag{4}$$

where γ_f is the instantaneous per-unit field voltage. The general solution of (3) yields

$$i_f = \gamma_f I_{f0} + Ke^{-\frac{t}{T'_{do}}}, \tag{5}$$

where K is a constant depending on the initial field current value. The damper cage effects are neglected, as they only affect the very first instants of electromagnetic transients. During the on-load operation, the contribution of stator currents needs to be taken into account. As result, the time constant during on-load operation takes a value which, to a first approximation, can be assumed equal to the short-circuit time constant T'_d [50].

A. EXCITATION CURRENT DYNAMICS

The ceiling voltage is the maximum voltage that can be provided by the ES under defined conditions [43]. The per-unit value of the ceiling voltage, with respect to the rated field voltage, will be indicated as γ_{ceil} below. An ideal ES must be able to apply the ceiling voltage instantaneously, in order to produce the fastest possible change in its excitation current. Based on the solution of (5), Fig. 2 shows the impact of the available ceiling voltage γ_{ceil} on the step response for a typical dynamic performance test [18], [51]–[54]. The ideal response is shown, where the step change of the field voltage is instantaneous [43]. A frequency response test is an alternative test, which will provide similar dynamic information about the ES [55].

In practice, the voltage applied to the winding reaches its maximum (ceiling) value in a finite time, which depends on the AVR response delay and on the circuitry between the AVR and the field winding according to the architectures that will be described in the following sections. Any ES is classified as high initial response (HIR) when it can reach 95% of the difference between ceiling voltage and rated field voltage in 0.1s or less under specified conditions [43].

Naturally, the higher the ceiling voltage, the faster the current response will be. However, the ceiling voltage amplitude is limited by various factors and, in particular, by the voltage withstand capability of the field winding insulation [17].

In the example shown in Fig. 2, the field current is supposed to be initially at 95% of its no-load value, i.e., $i_f(0) = 0.95I_{f0}$, and it is supposed that the ceiling voltage is applied to the field to increase the field current to a new set-point value of 1.05 pu. In such case, the particular solution to (5) is:

$$\frac{i_f}{I_{f0}} = \gamma_{ceil} + (0.95 - \gamma_{ceil})e^{-\frac{t}{T'_{do}}}. \tag{6}$$

The time Δt taken by the field current to reach the set-point value of 1.05*pu* in the open-circuit conditions, normalized with respect to the open-circuit time constant, is:

$$\frac{\Delta t}{T'_{do}} = \ln\left[\frac{0.95 - \gamma_{ceil}}{1.05 - \gamma_{ceil}}\right]. \tag{7}$$

Fig. 2 shows the field current response for various possible values of the per unit ceiling voltage γ_{ceil} from 1.5 to 4. It can be noticed from the figure that the field current dynamics is strongly affected by the ceiling voltage if the latter is low, but much less for ceiling voltage values above 2 times the rated field voltage. In other words, the speed of response is strongly dependent on the ceiling voltage for lower values, but less dependent for values of γ_{ceil} above 2 per unit.

Eqs. (6) and (7) can be modified for on-load conditions by replacing T'_{do} and I_{f0} by T'_d and I_f. In fact, the same considerations as for the no-load operation can be made. The use of T'_d rigorously applies to short-circuit conditions, but is also useful to describe the on-load step response dynamics to a first-order acceptable approximation [50].

Fig. 2 presents normalized (per unit) quantities. As a result, it applies to both no-load and on-load conditions. For the latter case, it is worth recalling that the base field voltages and currents u_f and i_f under nominal load are typically 1.5 to 2 times their no-load values.

B. DE-EXCITATION METHODS AND DYNAMIC RESPONSES

The same analytical approach discussed in the previous subsection can be employed for analyzing step responses of the field current in the opposite direction, i.e. when the field current has to be reduced or extinguished. However, in this case, the available negative ceiling voltage that can be applied to force the field current to zero may be slightly less than the positive one for certain types of ESs, as discussed in more detail below.

The de-excitation response is an important property of an ES. The energy stored in the field winding must be dissipated as fast as possible in case of a normal or forced stop. In fact, since the field winding is a highly inductive circuit, a sudden

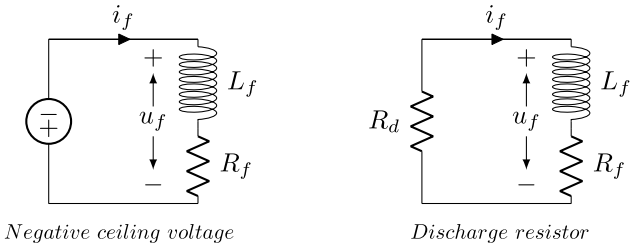

FIGURE 3. Simplified de-excitation circuit of the two main demagnetization methods.

interruption of the current flowing through it (i.e. by opening a breaker) would result in dangerous over-voltages that may exceed the field insulation withstand capability. Therefore, de-excitation is mandatory to reduce the field current to approximately zero before switching off the ES.

As discussed in the next section, the capability of quickly extinguishing the field current depends on the technology and, in particular, is a peculiar strength of static ESs when compared to brushless ones. A fast-response demagnetization is obtained either by feeding the field winding with a negative field voltage or short-circuiting it with a parallel-connected discharge resistor. Both methods are illustrated in Fig. 3.

1) DE-EXCITATION BY NEGATIVE CEILING VOLTAGE

When the WFSM operates at on-load condition, a negative ceiling voltage results in a normalized de-excitation current response described by (8), where $\gamma_{ceil,neg}$ is the applied negative ceiling voltage. The time $T_{37\%}$ taken by the field current to reach 37% of the nominal value is as in (9).

$$\frac{i_f}{I_f} = \gamma_{ceil,neg} + (1 - \gamma_{ceil,neg})e^{-\frac{t}{T'_d}} \tag{8}$$

$$\frac{\Delta T_{37\%}}{T'_d} = ln\left[\frac{1 - \gamma_{ceil,neg}}{\frac{1}{e} - \gamma_{ceil,neg}}\right] \tag{9}$$

Equation (9) is normalized with respect to T'_d since the on-load operation is typically the case of interest when evaluating the de-excitation performance. If the no-load de-excitation time is considered, T'_{do} must be used and $\Delta T_{37\%}$ takes a larger value. $\Delta T_{37\%}$ is often imposed by some standards or regulations not to exceed a given threshold as a safety-critical requirement [56]–[58]. Fig. 4 shows how the de-excitation time varies for negative ceiling voltages between 2 and 4 pu.

2) DE-EXCITATION BY DISCHARGE RESISTOR

A discharge resistor is a safety device designed to shorten the time needed to extinguish the field current. A short-circuit of the field winding by the discharge resistor under load conditions leads to a de-excitation time constant given by (10), where R_d is the discharge resistance. The field current dynamics will be then governed by (11) when starting from an initial field current equal to 1 per unit.

$$\tau_d = \frac{T'_d}{1 + \frac{R_d}{R_f}}, \tag{10}$$

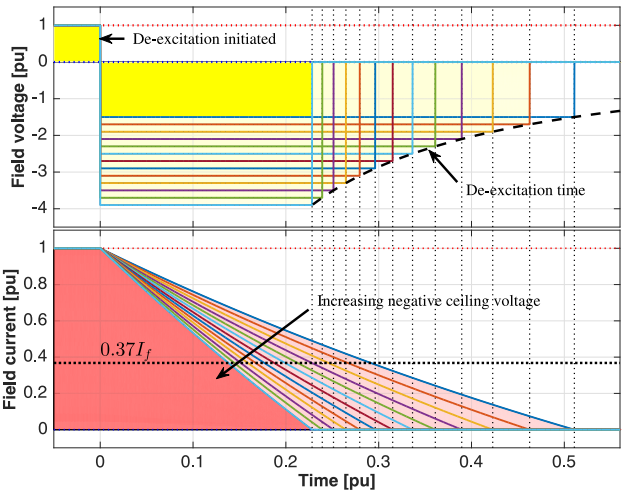

FIGURE 4. Illustration of an ideal de-excitation field current response from 1*pu* to 0*pu* for several negative ceiling voltage values. The time is normalized with respect to T'_{do} for no-load condition and to T'_d for on-load condition.

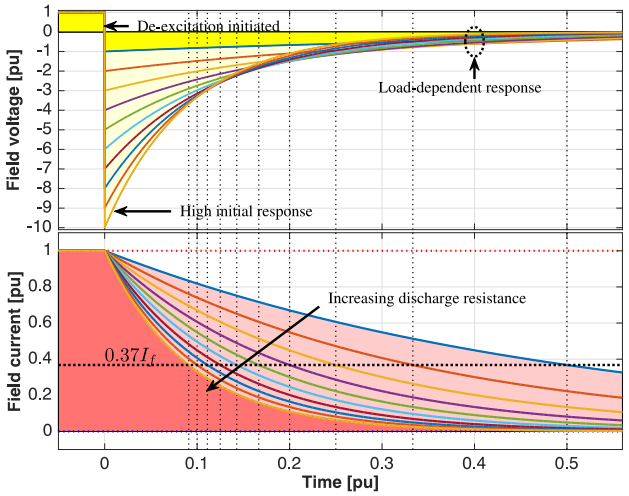

FIGURE 5. Illustration of an ideal de-excitation field current response from 1*pu* to 0*pu*, for several ohmic values of the discharge resistor, increasing from $\frac{R_d}{R_f} = 1pu$ to $\frac{R_d}{R_f} = 10pu$. The time is normalized with respect to T'_{do} for no-load condition and to T'_d for on-load condition.

$$\frac{i_f}{I_f} = e^{-\frac{t}{\tau_d}} = e^{-\frac{t}{T'_d}(1+\frac{R_d}{R_f})} \tag{11}$$

Moreover, $\Delta T_{37\%}$ decreases as the discharge resistance grows according to (12):

$$\frac{\Delta T_{37\%}}{T'_d} = \frac{1}{1 + \frac{R_d}{R_f}}. \tag{12}$$

Fig. 5 represents how the de-excitation current response changes for discharge resistances varying from $R_d = R_f$ to $R_d = 10R_f$. The diagram shows that a discharge resistor having a high resistance value compared with the field winding would be able to generate high initial de-excitation voltages. For this reason, in practice, the field winding insulation limits the maximum discharge resistance that can be used.

TABLE 1. Summary and comparison of the static excitation systems.

Method	Adopted technique	Merit	Weakness	Reference
A1: Potential source	Feeds excitation power from the generator bus by a potential transformer	Simple; robust; classical solution	Sensitive to bus voltage; needs over-dimensioning	[66]
A2: Compound source	Combines the contribution of potential- and current transformers	Provides sufficient fault current in weak grids	High investment costs; space usage; complex circuitry	[65], [68]
A3: Hybrid PMSM	Contribution of both PMs and coils in the rotor	Self-excitation capability	Expensive and complicated WFSM design	[69]
A4: Booster	A bypassed circuit provides an extra boost voltage from an ultra-capacitor	Field forcing under fault ride-through events	Based merely on additional equipment to the static exciter	[19]
A5: Boost-buck	A boost converter step provides extra field voltage under low bus voltages	Boosts the available; field voltage in a buffer	Expensive solution for large SMs	[70]–[72]
A6: Voltage source	A voltage source converter (VSC) provides flexible source voltage of the exciter	Forced excitation stability; avoids commutation failure	The system has many active components; expensive	[73]

The maximum de-excitation voltage also influences the choice of the field circuit breaker or excitation interruption devices as described in detail in [17], [56]. Considering all these restrictions, practical values of R_d/R_f usually lie between 0.5 and 2.0 [57]. As an alternative to conventional resistors, metal oxide or silicon carbide varistors are a good solution to reach faster de-excitation times with limited over-voltages. These are often referred to as non-linear discharge resistors, due to their non-linear voltage vs. current characteristic.

III. EXCITATION SYSTEM TECHNOLOGIES AND THEIR EVOLUTION

As shown in Fig. 1, the first ESs were based on DC exciters [59]. These use DC generators as a power source, driven by a separate motor or by the main alternator shaft, and supply DC current to the field through slip rings. DC excitation methods represent early commercial systems (from the 1920s to the 1960s) and have, by now, a merely historical value, as they have been superseded by AC exciters. The most commonly employed ESs since the 1960s can be classified into three categories: static, brushless and embedded (or integrated) systems. These three categories will be discussed in the next subsections in more detail.

A. STATIC EXCITATION SYSTEMS

Static exciters are dominantly used for large synchronous generators with power ratings in the order of several MVAs, which need to satisfy standardized technical requirements in terms of dynamic performance [43]–[45]. Figure 6 illustrates a classic example of this type of system. It includes two six-pulse SCRs bridges (i.e. SCR1 and SCR2 in the figure) connected in parallel to the WFSM field circuit, each of them with its own rectifier controller (C1 and C2). In this configuration, the SCR bridges usually operate in 'hot standby', i.e. one of them conducts the full excitation current, while the other remains in standby. When a failure occurs in the active bridge, then it is automatically disabled and the standby one takes over without any manual intervention. As an alternative approach, active current sharing between the rectifiers of these systems has been proposed [60]–[64]. The other elements in the system are the field discharge (FD) system, the field circuit breaker (FCB) and the AVR, which outputs the commands to the SCR bridge controllers in order to maintain the main machine voltage at its desired value through a feedback control loop.

The two classical types of static exciters, namely the potential source and the compound source, are illustrated in Fig. 7 [65], while, Fig. 8 presents some recently developed or proposed static systems. In addition, Table 1 compares all these static topologies and summarizes their main features.

Static exciters perform the de-excitation task by applying negative ceiling voltage obtained by controlling SCRs with a firing angle above 90° or through a discharge resistor. The latter is a passive component that can operate independently of the ES supply and it is often required, as it provides a reliable and independent de-excitation in case of severe failure of the AVR or faults within the SCR bridges [56].

1) POTENTIAL SOURCE (A1)

The potential source or bus-fed ES is the most popular choice in the power industry [66]. Topology A1 in Fig. 7 illustrates its main components, including brushes and slip rings, which represent the interface between the rotating and the stationary domains, the potential transformer (PT) and the six-pulse SCR bridge. The PT steps down the three-phase voltage from the generator terminals and feeds the SCR bridge. The latter rectifies the three-phase voltage and supplies DC current to the field winding. The rectifier output voltage amplitude is controlled by the AVR to achieve its multiple regulation purposes, such as control of the terminal voltage, limitation of field and terminal currents, reactive power exchange with the grid, generator load angle restriction and power system stabilization.

The ceiling voltage of the potential source exciter is very sensitive to the bus voltage. As a result, the PT secondary voltage should be carefully chosen to satisfy the dynamic requirements on the grid-side. The six-pulse SCR can attain 95% of the available ceiling voltage in less than 0.1 seconds and is thus considered a HIR ES [44]. A fast inherent response is essential for power system transient stability [67]. As previously mentioned, a discharge resistor (Sec. II-A) is

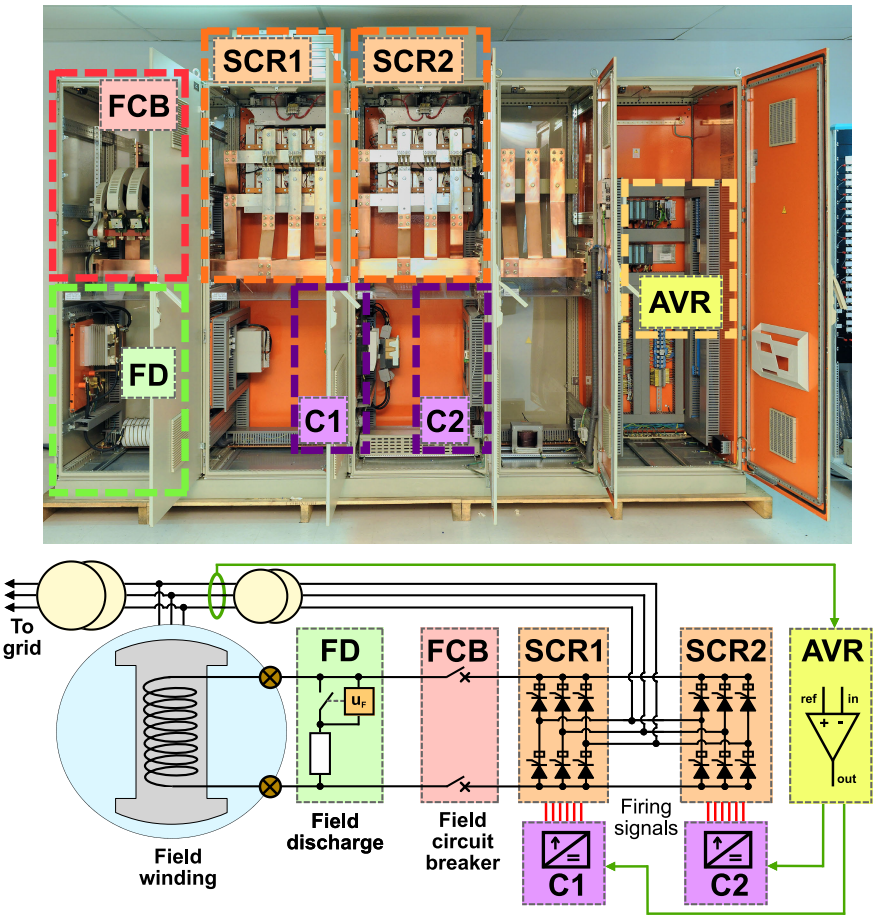

FIGURE 6. Components of a static excitation system for a 45 MVA, 514.3 *r*/*min*, 13.8 kV, 60 Hz synchronous generator (Courtesy of *Voith Hydro*).

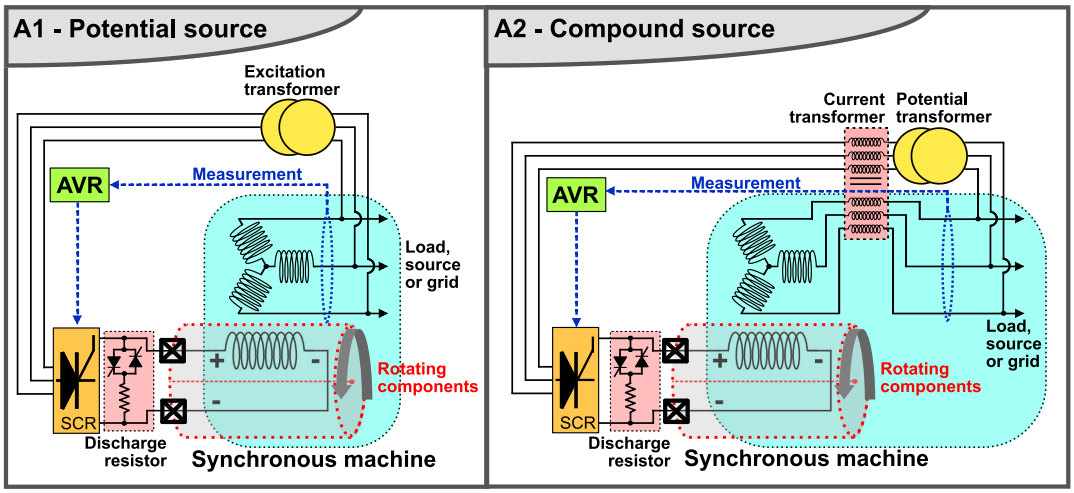

FIGURE 7. The two classical static excitation configurations.

usually connected to the SCR bridge output to ensure fast de-excitation (Sec. II-B).

2) COMPOUND SOURCE (A2)

The compound-type static ES combines the generator terminal voltage and the contribution from the phase currents via current transformers (CTs), as illustrated in topology A2 in Fig. 7. During a fault, the PT will not be able to sustain the excitation voltage. However, the fault current will provide excitation power via the CTs to compensate for this. The compound system is an ingenious way to overcome some of the disadvantages of the potential source excitation. Its use is

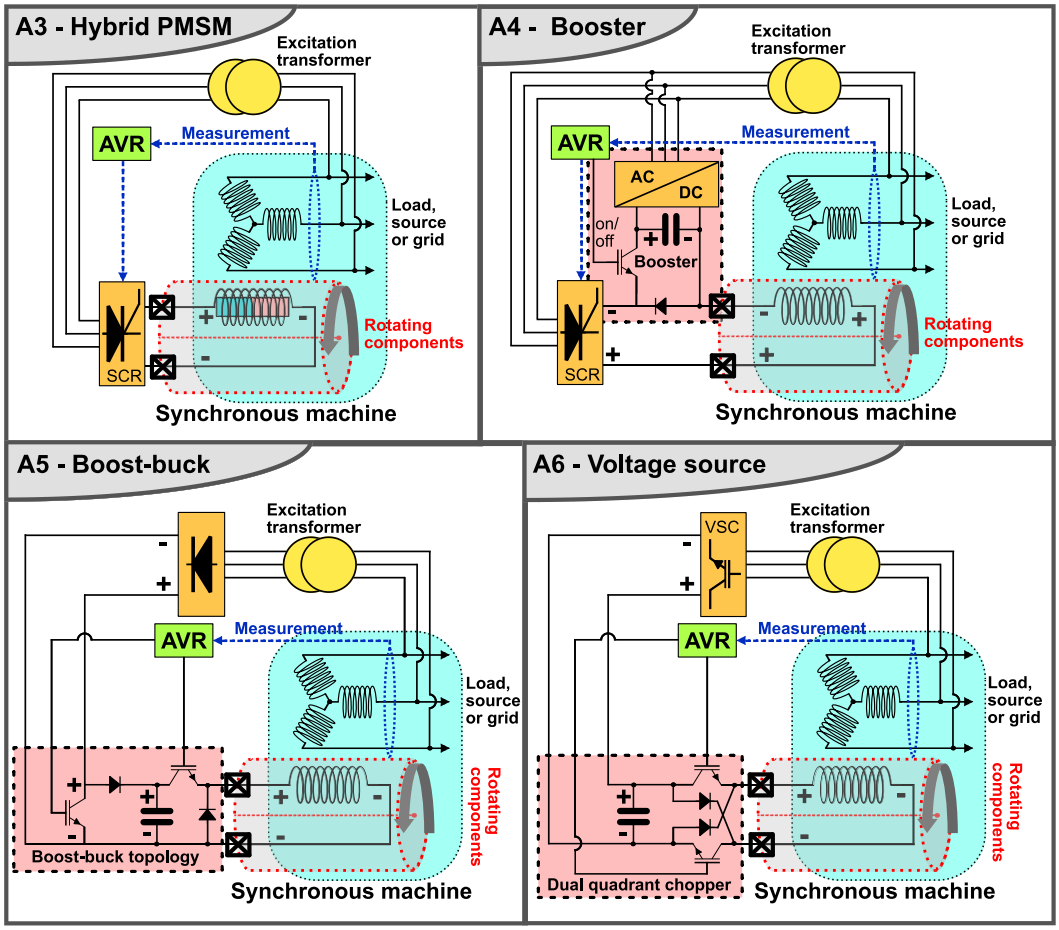

FIGURE 8. Modern extensions of the static excitation system, from community research and the industry.

particularly recommended in low-inertia systems. Examples of those are isolated grids, e.g., shipboard power systems [68] or industrial plants, or large generators connected to relatively weak grids, where the voltage cannot be sustained by other sources in the presence of a fault [44]. High investment costs and complex circuitry are some of the main drawbacks of the compound technology, and an alternative solution is to design the potential source system with a higher ceiling voltage [65], whenever this is technically feasible and economically convenient. In order to overcome the limitations of systems A1 and A2, alternative solutions are proposed in the recent literature, and new solutions have been tested by manufacturers. These are described in the next subsections.

3) HYBRID PMSM (A3)

The hybrid-type static exciter is the topology A3 in Fig. 8. In this arrangement, the PMs installed on the rotor of the generator provide the rated flux to the machine at no load. The field winding is, instead, used to compensate for the armature reaction during on-load operation [69]. As a result, the hybrid system could be classified as a PM synchronous machine with armature reaction compensation. The self-excitation capability has obvious advantages in islanded operation and in presence of weak grids, thanks to the relatively low excitation current that is required. However, the need for PMs makes the generator design more complicated and expensive.

4) BOOSTER (A4)

The static excitation booster, i.e., topology A4 in Fig. 8) is intended to improve the fault ride-through capability of the classical potential source exciter [70]–[72]. The DC-link ultra-capacitor is normally bypassed by a diode. During a voltage sag event, the insulated-gate bipolar transistor (IGBT) is activated and the ultra-capacitor is connected in series with the output of the SCR bridge. This is another example of a tailor-made solution to overcome some limitations of the potential source excitation aiming to improve the transient stability of the power grid [51]. Note that the topology A4 is different from the 'transient excitation boosting' system proposed in the early 1990s [74], which consisted of very powerful static exciters.

5) BOOST-BUCK (A5)

The boost-buck chopper configuration of the static ES is shown in Fig. 8 as topology A5 [75] in one of its possible implementations. It is another alternative to solve the field forcing capability of potential source systems in fault or low grid voltage conditions. This configuration employs a

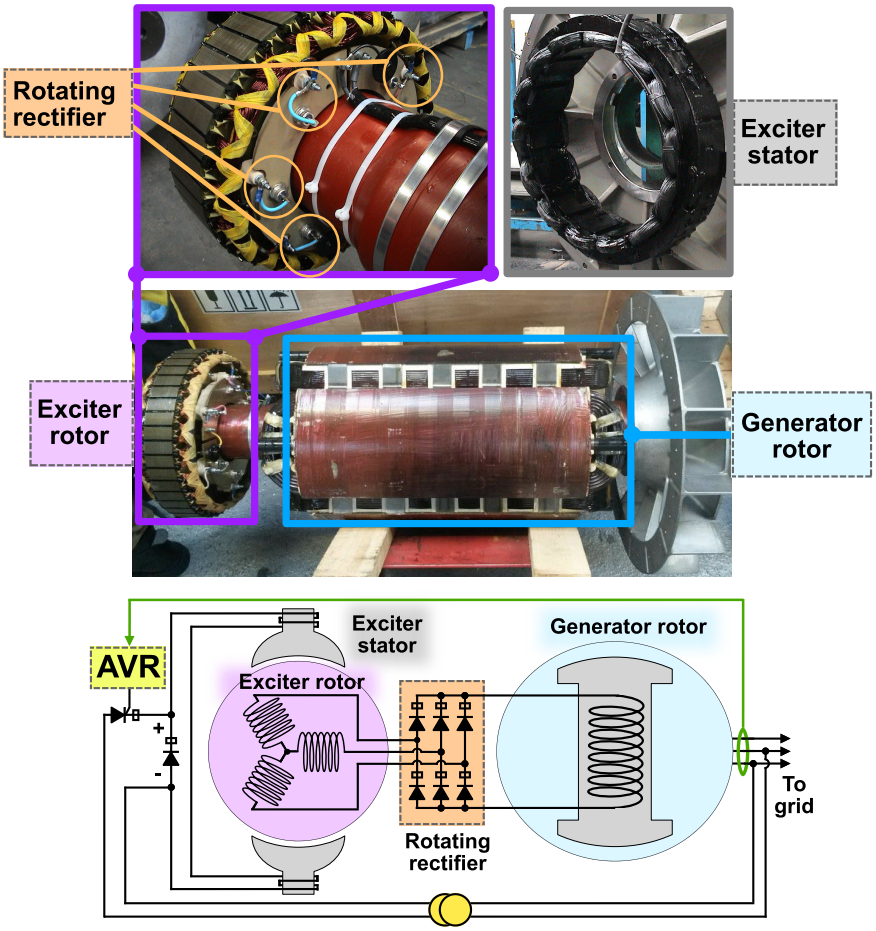

FIGURE 9. Components of a brushless excitation system for a 400 kVA, 1500 *r*/*min*, 400 V, 50 Hz (175 Hz for exciter) synchronous generator.

boost-buck converter which can always provide the DC-link ceiling voltage at its output even when the terminal voltage is temporarily suppressed. This is possible thanks to the DC-link capacitor acting as an energy buffer that prevents transients in the power supply from immediately affecting the ES output.

In addition, unlike an SCR bridge, the boost-buck configuration can turn off its switches at any given instant and synchronization of its controller to the grid voltage is not necessary. This allows the ES to be fed by almost any available power supply, including a pilot machine, the AC auxiliary system, or even the DC auxiliary system. As an example, [75] proposes the boost-buck topology (shown in Fig. 8-A5) fed via an excitation transformer and a three-phase diode bridge. The solution is expected to be expensive for large synchronous generators, which demand a high direct current to be fed by a diode rectifier together with other power electronics apparatus. The compact thyristor based topology (Fig. 6) is the most mature and well-established technology for those applications [76], [77].

6) VOLTAGE SOURCED (A6)

In Fig. 8, topology A6 illustrates a static exciter with a front-end VSC and an output dual-quadrant chopper [73]. The presence of a DC-link voltage and capacitance (with short-term energy storage capability) provides a stronger field forcing capability which strengthens the transient stability of the WFSM. In addition, the VSC can operate in boost mode and the output chopper provides a faster field voltage response compared to the SCR bridge.

The de-excitation process starts immediately by interrupting the PWM signals at the H-bridge chopper output. As a result, it eliminates a possible commutation failure by the use of IGBTs. Typically, there are challenges in designing a totally passive, fail-safe trigger circuit for the discharge resistor as recommended in [44]. Considering that the field winding energy can reach several *MJs* in large generators, the DC-link would require a large capacitor. However, the VSC typically controls the DC-link voltage and will actively discharge the capacitor during the de-excitation process.

B. BRUSHLESS EXCITATION SYSTEMS

The basic and most common structure of a brushless ES is illustrated in Fig. 9. It consists of a rotating exciter with a three-phase winding on the rotor, which is mounted on the main machine shaft. The exciter field winding is wound

TABLE 2. Summary and comparison of the brushless excitation systems.

Method	Adopted technique	Merit	Weakness	Reference
B1: Shunt	Utilizes a single line-to-line voltage of generator terminals	Simple; self-excited; power AVR from measured voltage	Sensitive to short-circuits disturbances and overloads	[83], [84]
B2: EBS	The shunt source is extended with an excitation boost generator	Can provide sufficient short-circuit current	Relies upon a backup EBS system	[85]
B3: PMG-SCR	Separately excited by a single-phase permanent magnet generator	Independent of WFSM terminals; high overload capability	PMG adds weight and complexity	[89]
B4: PMG-PWM	Separately excited by a three-phase permanent magnet generator	Low exciter field current ripple	PMG adds weight and complexity; PWM adds new critical components	[91]
B5: Auxiliary source	Auxiliary low-voltage grid source feeds a brushless exciter	Classical solution	Relies on an external auxiliary source and transformer	[24], [25] [93]–[96]
B6: Auxiliary winding	Excited by auxiliary winding located inside the WFSM stator slots	Eliminates need for a PMG; Independent of load type	Increased size of WFSM; needs initial PM flux	[97]
B7: Asynchronous exciter (AE)	VSC-fed asynchronous machine exciter feeds the WFSM	Delivers field current at standstill for high-torque start	Requires a complex VSC; to operate the AE	[109], [110]
B8: Rotating transformer (RT)	Single-phase rotating axial flux AE feeds the WFSM	Allows high frequency excitation for space reduction	Depends on high frequent switching of power electronics	[111]–[117]
B9: Shunt hybrid	Provides basic excitation from embedded PMs in the exciter stator	Does not depend on residual magnetism	Terminal voltage cannot be fully controlled from zero	[87]
B10: High-speed de-excitation	Self-actuated switches de-excites e the WFSM under internal faults	Improves the WFSM safety; avoids fault damaging	Need to install a discharge resistor on the shaft	[118]–[120]
B11: PME-SCR two-stage	A three-phase PM exciter feeds a thyristor-controlled rotor armature	Exciter stator is replaced by PMs	Field voltage is load dependent, high voltage drop in commutation	[37], [121]
B12: HSR dual-control	A rotating thyristor bridge rectifies a controlled WFSM field voltage	Same dynamic performance as static exciters	Needs active rotating components, wireless interface and dual control	[34], [35]
B13: PME-SCR hybrid-mode	A six-phase PM exciter feeds a a flexible thyristor topology	Can operate with a reduced stationary loading of the exciter	Needs many active components installed on the shaft	[122], [123]
B14: PME-passive rotating chopper	A three-phase PM exciter feeds a rotating diode bridge with a chopper	Few active rotating components	Requires a robust rotating capacitor; weak de-excitation	[36], [124]
B15: CPT	Capacitive electrodes transfer excitation power to the WFSM rotor	Simple; compact	Restricted to low-power excitation applications	[125]–[127]
B16: PME-VSC	A rotating VSC feeds a rotating DC-link and a chopper	Excellent de-excitation performance	Many active rotating components; needs a rotating capacitor	[128]

around stator poles and is supplied by a DC source, although some AC-fed stator designs may be required in synchronous motors to provide field current at stand-still as discussed later on. When the shaft revolves, the main air-gap field induces electromotive forces and thus currents in the exciter rotor phases. A rotating AC-to-DC rectifier, assembled onto the exciter rotor, rectifies the induced AC current into DC current and feeds the rotor field winding of the main WFSM.

Traditionally, the use of a rotating exciter and a diode rectifier is considered unfit to deliver prompt field voltage control, as required for HIR ESs [78]–[80]. Moreover, until recently, the de-excitation methods described in section II-B have been regarded as unsuitable for implementation in brushless ESs. In contrast, the speed of response is not a stringent requirement in applications such as standby power, marine, oil and gas, UPS mobile constructions, etc. [81]. In those, generators ranging from few kVA to few MVA are often designed to feed mainly passive ohmic-inductive loads, for which AVR fast response and de-excitation capabilities are not major concerns. Not least, the use of slip rings and brushes is not allowed in potentially explosive environments, which limit their application. Furthermore, they demand constant maintenance due to mechanical wear and tear.

Owing to the above, brushless exciters represent a good solution for applications requiring flexible excitation control, limited maintenance and operational costs. As such, they nowadays represent the most common configuration applied by industry in small-to-medium generator sets [82]. Fig. 10 presents the classical brushless ESs as well as new topologies introduced in recent times, or still under development and research. Finally, Table 2 compares all the brushless topologies taken into account by this work.

1) SHUNT (B1)

The shunt-connected brushless exciter is a self-magnetized system [83], shunted on the WFSM terminals. It uses the single line-to-line voltage of the generator terminals to power the AVR [84]. The same output is measured and used as a feedback signal to regulate the generator voltage. The approach is cheap and simple to implement. However, the AVR supply power is very much dependent on load-side events such as voltage disturbances and faults. Also, when non-linear loads (e.g. power electronics based loads such as PCs, fluorescent lamps and inverter-fed motors etc.) are fed by the main generator, the AVR supply power quality is compromised [82]. The solution cannot tolerate high overloads, neither can it offer sustained short-circuit operation capability. In the worst case of a short-circuit fault occurring in the proximity of the machine terminals, the voltage may drop to zero and powering the AVR would become challenging if no precautions are taken. Apart from the mentioned issues, the shunt solution is the simplest and cheapest among the brushless systems described in this section. The excitation method is typically implemented in WFSMs rated up to 700 kVA, but it is not uncommon for several MVAs as well.

2) EBS (B2)

The excitation boost system (EBS) is a boosted version of the shunt-type ES. A small excitation boost generator is installed on the WFSM shaft to power the excitation boost controller (EBC), which is an extension of the classical AVR [85]. The EBS has its terminals connected in parallel to the output of the main AVR and is activated by an AVR command. The EBS only intervenes when needed, e.g., in case of faults, load injections, etc. allowing the required excitation power to be developed even under these circumstances. It is not widespread in applications that require continuous power generation, but more common in emergency, back-up or safety-critical applications. Moreover, it is compatible with non-linear loads such as power electronics based devices and motors at startup and can provide excitation for 300% sustained short circuit current or more.

3) PMG-SCR (B3)

The PMG-type system is a separately-excited arrangement, as opposed to the classical self-excited shunt-type topology [86]. It employs an auxiliary electrical machine, the PMG installed at the end of the WFSM shaft, to provide power to the AVR when the shaft is running [87], [88]. The AVR power is completely independent of the WFSM terminal voltage and of the type of load it supplies. Another major advantage compared to the self-excited shunt topology is that the PMG provides more reliable power to the AVR and safer voltage build-up, which does not rely on residual magnetism but is assured by the PMs. Furthermore, it enjoys a high overload capacity and is suitable for demanding applications. In the SCR-type of the PMG system, the PMG is equipped with a three-phase stator winding connected to a 4-pulse diode bridge rectifier which, in turn, feeds a single SCR device. Only two phases of the PMG are utilized in this case, thus avoiding the design of a dedicated single-phase PMG. By acting on the SCR firing angle, the AVR adjusts the supply voltage applied to the rotating exciter stator terminals. A freewheeling diode connected in anti-parallel with the SCR ensures that the exciter supply current can flow while the SCR is in blocking mode. The switching frequency of the SCR is two times the fundamental electrical frequency of the PMG stator. As a result, rapid dynamics for the exciter supply voltage is difficult to obtain [89]. However, a simple droop control of the AVR can be easily implemented [90]. The PMG-type is the most common ES for non-linear loads, in applications where the grid voltage is affected by significant disturbances typically due to power electronics devices and motor starting. The PM machine obviously adds weight and overall complexity to the system. As a result, it is mostly used for medium-size generator sets rated between 700 kVA and 4 MVA.

4) PMG-PWM (B4)

The PWM-type of the PMG ES employs a three-phase PMG that supplies a DC-link capacitor via a 6-pulse diode rectifier [89], [91], [92]. An IGBT regulates the exciter stator current using PWM technique [91]. In general, it is a variant of the PMG-SCR topology, thus offering similar benefits. However, it provides a higher power quality to the exciter stator winding since PWM harmonics have higher frequencies and are thereby attenuated by the exciter winding inductance, resulting in less current ripple than in the PMG-SCR case.

5) AUXILIARY SOURCE (B5)

The auxiliary source brushless ES [25], [93]–[95] is a classical solution for large grid-connected WFSMs, where the stator winding of the main exciter is fed from an auxiliary low-voltage grid available for the ES. The main exciter could also be fed by the main grid via an excitation transformer and a thyristor rectifier [96]. The solution is simple and robust, but implies the availability of a suitable auxiliary power source or of a strong main grid. In safety-critical nuclear power applications, an exclusive exciter with 39 phases can be used to improve the reliability and fault tolerance of the ES [24], [96].

6) AUXILIARY WINDING (B6)

The auxiliary winding solution is characterized by the use of an auxiliary, single-phase winding located inside the WFSM stator slots [97]. The single-phase winding is connected to an isolating transformer that feeds the exciter stator winding through a single SCR device controlled by the AVR. When the WFSM operates at no load before synchronization to the grid, an initial excitation must be provided. For this purpose, PMs embedded in the exciter stator are used. The auxiliary winding based ES is less common than the previously described ones and is typical of power ratings between 4MVA and 15MVA. This excitation method provides power to the AVR independently of the load type, as in separately-excited systems (i.e., equipped with PMG). However, the voltage induced in the auxiliary winding is produced by the main air-gap flux and therefore depends on the WFSM operating condition. For this reason, the design of this kind of ES is a challenging task. The auxiliary winding eliminates the need for the PMG, thus resulting in a very cost-effective solution. On the other hand, the additional auxiliary winding reduces the useful space for installing the main stator three-phase winding, potentially resulting in an increased size of the WFSM. Note that there are possibilities for using more auxiliary windings. In the field of synchronous motors, they can be employed to obtain a bearing-less configuration [98], [99].

7) AE (B7)

Wound-rotor synchronous motor for variable-speed drives tends to employ AEs [100]. Moreover, civil aircrafts use electrically excited generators for fixed speed and variable speed applications [101], [102]. The exciter behaves as a three-phase rotating transformer. As a result, it can deliver field current to the main WFSM even at standstill conditions. In high-power variable-speed drive applications, the AE is

traditionally fed by an AC/AC anti-parallel thyristor converter, due to economic constraints, while the main stator is usually fed from either a current-source or voltage-source inverter. Due to the high complexity of the system, efficient modeling has been proposed [103]. Moreover, measurement of the field current is not straightforward without brushes and slips rings or without fast wireless data transmission. As a result, field current estimation and control methods have been a research focus [104]–[106]. Good accuracy in the field current estimation ensures superior dynamic and steady-state performance. In addition, estimation of the rotor position by high-frequency voltage injection and by model based approaches have recently been addressed [107], [108]. Two-phase AEs have also been proposed in integrated starter/generator applications [109], where the motor operation capability removes the need for a separate starter, such as in aircraft onboard generators. The AE can provide field current for full load starting of the main WFSM when the rotor is at standstill.

Figure 8 shows the AE with an auxiliary source. However, the AE system could also work with a pre-exciter PMG configured in a three-stage system [110].

8) RT (B8)

The rotating transformer (RTs) electrically-excited configuration is a competitive choice in vehicle applications for deep flux weakening, high torque and efficiency at low speeds [111], [112]. The RT based brushless exciter is essentially a single-phase AE in the axial rotary configuration. However, it can also be designed in a pot core configuration [113]–[115]. It has a passive 4-pulse diode bridge rectifier in the rotor and an active-switch power electronics supply for the exciter stator winding. The use of high frequencies for the exciter stator supply has been shown to be beneficial for compactness in vehicle applications [116], enabling wireless power transferring technology [117]. The cost and supply volatility of rare-earth PMs have intensified the interest for RT based WFSMs in vehicle applications [112].

9) SHUNT HYBRID (B9)

To overcome the limitations of the shunt excitation method without resorting to a separate PMG solution [87], a hybrid excitation for the exciter is presently under investigation and development. The PMs are installed in the exciter stator in order to provide the "basic excitation power" to the main machine during its no-load operation. In this way, there is no need to modify the circuitry feeding the exciter and/or the generator field windings. This solution can lead to a significant field loss reduction in the exciter in any loading condition of the WFSM, thus resulting in improved thermal management of the system. In addition, the PMs ensure continuous operation of the system even in case of a fault occurring in the exciter field winding, thus improving the overall reliability. Also, the voltage build-up process during starting is improved with this solution, as it does not rely upon the ferromagnetic core residual magnetism as in the shunt excitation method. However, the WFSM terminal voltage cannot be fully controlled from zero at rated speed, which is needed for ESs employed in test-field applications. The SCR based AVR compensates for the armature reaction under loaded conditions.

10) HIGH-SPEED DE-EXCITATION (B10)

One of the main drawbacks of the conventional brushless ESs is the difficulty of implementing the de-excitation strategies addressed in Section II. Recently, multiple tests have been carried out to provide a self-actuated high-speed de-excitation system for the conventional brushless arrangement in large power plants [50], [118]–[120]. A non-linear discharge resistor is usually bypassed in the rotor circuitry but is activated during internal short-circuits to avoid damages to the machine.

11) TWO-STAGE PME-SCR (B11)

In this configuration, the stator winding of the main exciter is replaced by a PMs, yielding an outer pole PM exciter (PME) [37], [121], [129]. Two-stage means that there are only two machines involved, i.e., the exciter and the generator. All control actions are accomplished by the SCR mounted on the rotor. This technology has similar characteristics as the HSR dual-control, except for the fact that the ceiling voltage cannot be controlled due to the presence of PMs in the exciter stator. As a result, the available ceiling voltage of the ES will be directly dependent on the loading condition of the WFSM. This is because the WFSM loading is reflected in its field current, causing a high commutation voltage drop across the rotating SCR rectifier. Moreover, a high ceiling voltage demands a high SCR rectifier firing angle, which has been shown to generate torque pulsations resulting in possible damages to the exciter stator [129].

12) HSR DUAL-CONTROL (B12)

The high-speed response (HSR) dual-controlled ES is a commercial product for large SMs [34], [35]. A rotating 6-pulse SCR bridge rectifier is remote-controlled through a wireless system and mounted on the rotor as an interface between the exciter armature and the generator field winding. The solution performs two control tasks: 1) exciter field current regulator (FCR) on the stator side; 2) AVR on the rotor side. It features the same dynamic performance of the conventional static ES, but without the need for brushes and slip rings. In contrast, it is not directly sensitive to the generator terminal voltage as the static systems. The ceiling voltage amplitude can be controlled by the FCR, only depending on a low-power auxiliary source, typically fed from a low voltage grid.

13) PME-SCR HYBRID-MODE (B13)

The PME-SCR hybrid mode configuration is a multiphase extension of the PME-SCR two-stage system [38], [122]. It utilizes a dual-star PM exciter with a 12-pulse SCR rectifier, composed of two rectifier units connected in either parallel

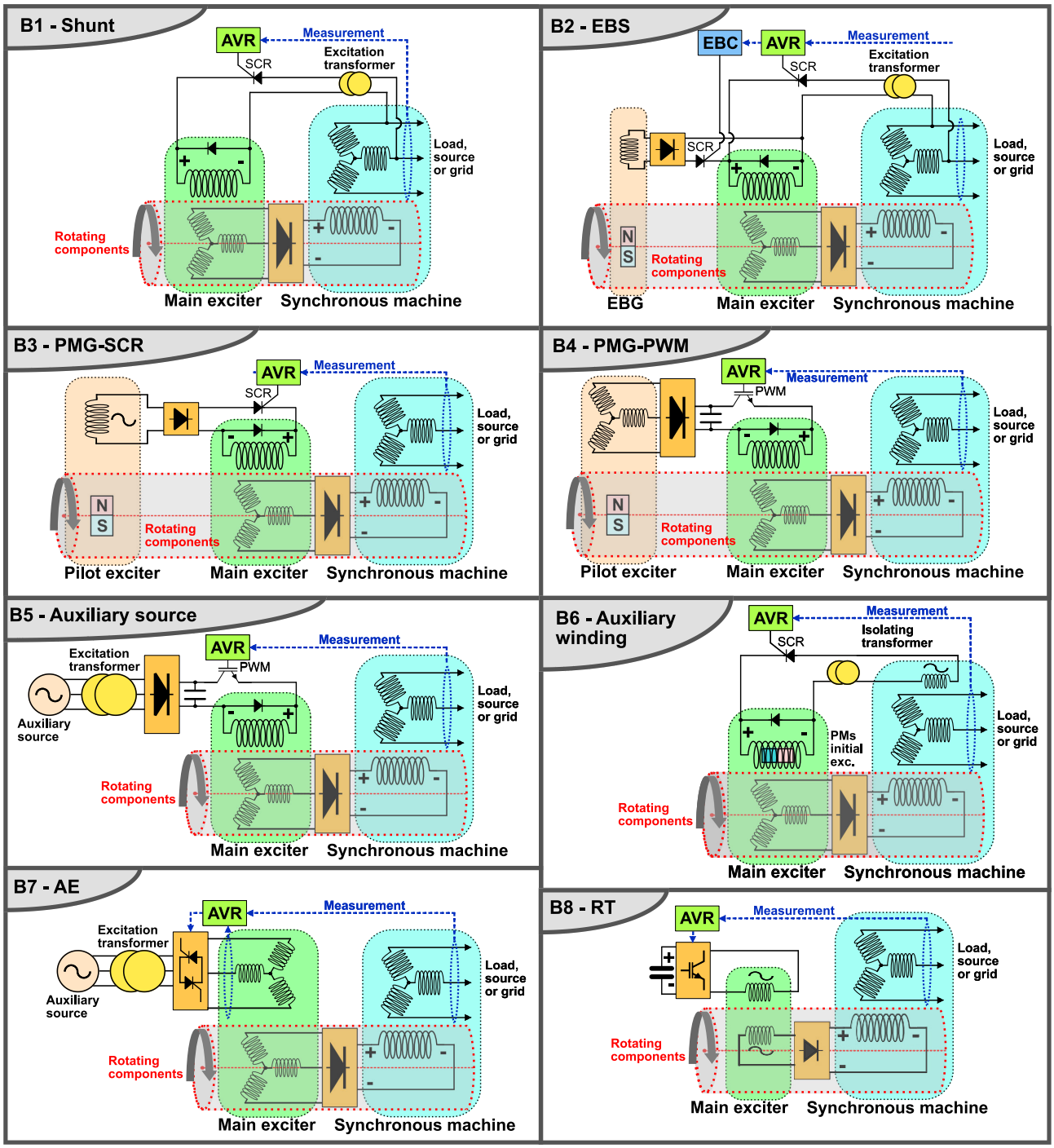

FIGURE 10. Overview of the classical brushless excitation configurations.

or series. The hybrid-mode topology typically works with a parallel connection in stationary conditions for low exciter currents, causing small torque pulsations. However, the series connection is activated with a single IGBT device to apply the full ceiling voltage to the exciter. The system also provides both active current sharing [123] and redundant post-fault operation for enhanced power production reliability [122].

14) PME-PASSIVE WITH ROTARY CHOPPER (B14)

There has been recent research trying to extend the classical brushless systems replacing the rotating diode bridge rectifier with a rotating thin film capacitor and a modern output chopper [36], [124], [130]. The system has the advantage of relatively few rotating active components. However, the DC-link capacitor must be designed to absorb the magnetic energy

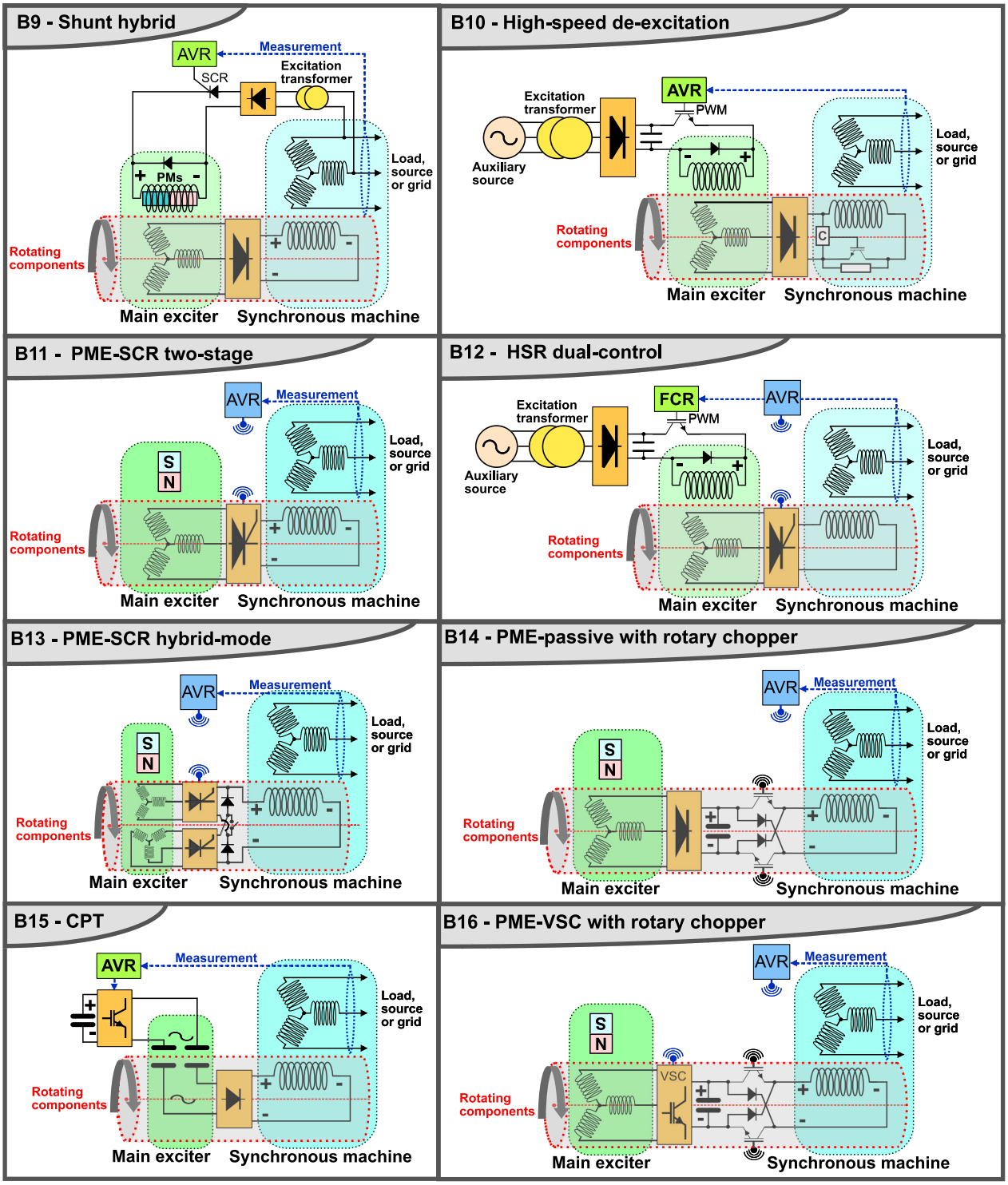

FIGURE 11. Modern extensions of the brushless excitation configurations, from community research and the industry.

stored in the field winding during a rapid de-excitation because the diode bridge is power-unidirectional.

15) CPT (B15)

Although RTs (B8) provide a viable contact-less solution, the use of a Capacitive Power Transfer (CPT) removes the need for additional windings and magnetic cores [125]. The CPT is based on a rotating capacitor with relative motion between electrodes having constant active surfaces and air gap between them. Due to the small coupling capacitance in air, the solution is suitable for low-power excitation applications [126]. However, hydrodynamic CPTs can provide a

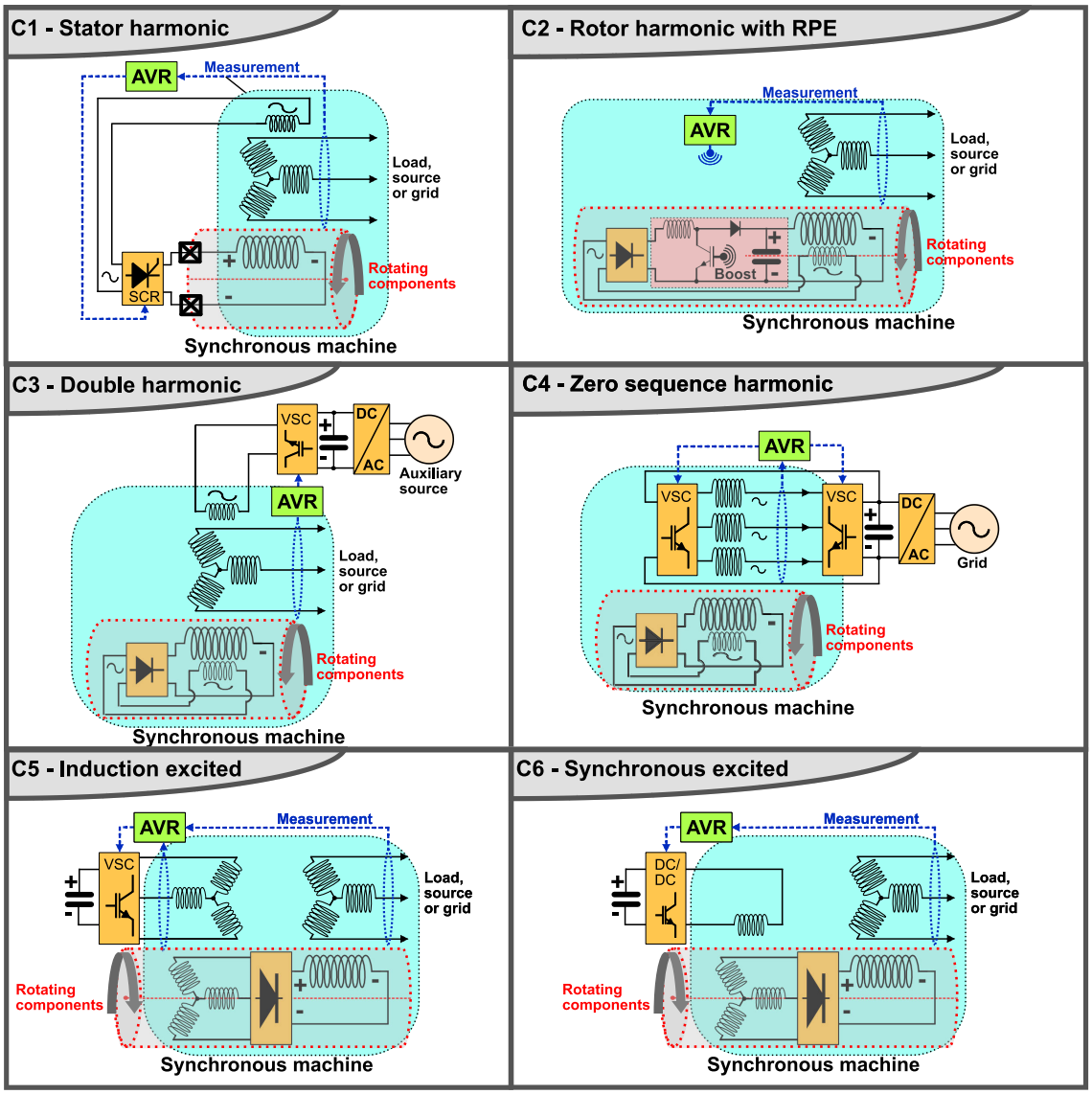

FIGURE 12. Embedded, integrated or exciterless excitation, both classical and modern.

larger excitation power [127]. Moreover, they represent an advantageous technology in terms of weight, volume and construction simplicity. [131].

16) PME-VSC WITH ROTARY CHOPPER (B16)

Finally, the PME VSC solution with a rotary chopper provides a full-scale modern power electronics solution. The chopper can demagnetize the field winding and the rotating VSC can de-energize the DC-link capacitor. As a result, the size of the rotating capacitor can be significantly reduced. As a drawback, the number of active rotary components increases [128]. Note that the rotating VSC control requires direct measurement or estimation of the rotor position.

C. EMBEDDED EXCITATION SYSTEMS

The embedded ES is an exciterless alternative where the exciter components are integrated into the main WFSM stator. Although the idea is old [136]–[145], new solutions and implementations have been recently proposed. Table 3 compares all the embedded topologies presented herein.

1) STATOR HARMONIC (C1)

The stator harmonic winding system is an old classical embedded system [132]. The excitation power is generated by an additional single-phase harmonic winding embedded in the stator of the main machine and designed so that air-gap space rotating field harmonics induce an electromotive force in it. This suffices to generate enough power to feed the rotor field winding via a 4-pulse SCR through brushes and slip rings [20]. From a conceptual point of view, it is similar to the solution B6 shown in Fig. 10, with its positive and negative sides. On the other hand, being an exciterless solution, the additional stator harmonic winding must be able to provide the full excitation power to the WFSM. This indicates that more space is necessary

TABLE 3. Summary and comparison of the embedded or exciterless excitation systems.

Method	Adopted technique	Merit	Weakness	Reference
C1: Stator harmonic	Embeds an additional harmonic winding into the stator structure	Simple; robust; few components	Increased size of WFSM; requires brushes and slip rings	[132]
C2: Rotor harmonic	Utilizes rotor damper slot harmonics to harvest excitation power in the rotor	Compact; brushless	Requires active rotating components and remote control	[133]
C3: Double harmonic	A stator harmonic winding energizes a rotor harmonic winding	Compact; brushless	Depends on an auxiliary source (VSC); increased size of WFSM	[20]
C4: Zero sequence	A stator harmonic winding energizes a rotor harmonic winding	Compact; high utilization of WFSM; brushless	Must be converter-fed; extra power electronic components	[19], [134]
C5: Induction excited	An induction machine embedded into the main WFSM structure	Excitation at standstill; brushless	Limited to cylindrical rotor; requires auxiliary VSC source	[21], [22]
C6: Synchronous excited	A synchronous machine exciter embedded into the main WFSM structure	Compact; brushless; low-power AVR	Limited to cylindrical rotor; cannot excite at standstill	[135]

for its allocation, thus resulting in a significant increase in the active WFSM size.

2) ROTOR HARMONIC WITH RPE (C2)

The exciterless system with rotating power electronics (RPE) embeds the whole ES circuitry in the rotor [133]. It utilizes rotor damper slot harmonics to induce the excitation power in a single-phase auxiliary circuit embedded in the rotor. The auxiliary winding injects current into a rotating DC-link via a boost converter stage, and the DC-link voltage feeds the WFSM field winding. This solution does not require brushes and slip rings.

3) DOUBLE HARMONIC (C3)

In the double harmonic system, a harmonic air-gap flux is generated by a stator auxiliary winding featuring a number of poles different from the main WFSM. This energizes an additional harmonic winding embedded in the rotor which feeds the field winding [20]. Although the technology has interesting features such as compactness, it depends on an auxiliary source to feed the stator harmonic winding via a VSC.

4) ZERO SEQUENCE (C4)

The zero-sequence system avoids brushes and slip rings via a converter-fed stator that generates a zero-sequence harmonic component that excites a harmonic winding embedded in the rotor, which is used to feed the field winding [19], [134]. The compactness of this system is a significant strength. However, it requires advanced power electronics, which adds costs [20]. A similar strategy utilizing sub-harmonic components has been recently proposed [146], [147].

5) INDUCTION EXCITED (C5)

The induction excited topology combines both an AE and the main WFSM into the same system. The main WFSM and the AE are designed with a different number of poles to avoid a magnetic coupling between them [21], [22]. Since the exciter is an induction machine, the WFSM field winding can be excited during standstill conditions, which makes it suitable for generator/starter applications and for high-end motor applications. The solution requires an auxiliary source that feeds the induction machine via a VSC.

6) SYNCHRONOUS EXCITED (C6)

In the synchronous excited topology, the main WFSM and a DC-fed brushless exciter are assembled together. They are configured for a different number of poles so that they do not interfere electromagnetically with each other [135]. The advantage is that this configuration can be excited by a single-switch DC-DC converter having a relatively low power rating.

IV. CONCLUSION

This paper has covered all the main ES categories presently implemented or proposed for WFSMs. A wide range of topologies for each category has been described, highlighting state-of-the-art technologies as well as recent trends. The design of an ES involves different performance challenges which are strongly influenced by the application at hand. These challenges include speed of response, de-excitation capabilities, field forcing requirements and starting performance. Additional open issues relate to compactness, simplicity, safety, operational costs and maintenance. The key features of the different technologies are summarized in Tables 1, 2 and 3.

In addition to traditional systems, new solutions are necessary to address the increasingly demanding performance requirements often imposed on modern WFSM, such as:

- post-fault operation for reduced downtime [122] and compensation of cooling discrepancies [123];
- extended capability diagram and over-excitation support under long-term voltage instability [148], [149];
- excitation boosting for enhanced power system stability [73] and voltage-sag ride through capability [70];
- cancellation of unbalanced magnetic pull [150], [151];
- mitigation of air-gap flux density harmonics [152], [153];
- faster high-torque starting by polarity inversion [154].

The overview presented in this paper on traditional and modern approaches to field excitation for WFSMs has shown that there are many options available and the selection of the best system architecture strongly depends on the specific application requirements. Classical static exciters are still

the preferred choice for most of large MVA generators, but new brushless exciters are being introduced and developed as competitive alternatives. Conventional brushless exciters are dominant for smaller WFSMs, but harmonic integrated exciters are paving the way to more compact solutions.

In addition, thanks to the recent advances in the field of rotating power electronics, and wireless rotor signal transmission and monitoring, ESs for WFSMs are expected to further evolve and meet new requirements and performance standards. In such a wide and fast-evolving scenario, this work represent a useful reference for designers and practitioners to identify the most suitable solution for a given application, especially in view of possible revisions of the current standards on voltage regulation and control.

REFERENCES

[1] K. Sedlazeck, C. Richter, S. Strack, S. Lindholm, J. Pipkin, F. Fu, B. Humphries, and L. Montgomery, "Type testing a 2000 MW turbo-generator," in *Proc. IEEE Int. Electr. Mach. Drives Conf.*, May 2009, pp. 465–470.

[2] *IEEE Standard for Salient-Pole 50 Hz and 60 Hz Synchronous Generators and Generator/Motors for Hydraulic Turbine Applications Rated 5 MVA and Above*, IEEE Standard C50.12-2005, Feb. 2006, pp. 1–45.

[3] R. J. Best, D. J. Morrow, D. J. McGowan, and P. A. Crossley, "Synchronous islanded operation of a diesel generator," *IEEE Trans. Power Syst.*, vol. 22, no. 4, pp. 2170–2176, Nov. 2007.

[4] J. Knudsen, J. D. Bendtsen, P. Andersen, K. K. Madsen, and C. H. Sterregaard, "Supervisory control implementation on diesel-driven generator sets," *IEEE Trans. Ind. Electron.*, vol. 65, no. 12, pp. 9698–9705, Dec. 2018.

[5] R. C. Schaefer, "Excitation control of the synchronous motor," *IEEE Trans. Ind. Appl.*, vol. 35, no. 3, pp. 694–702, May 1999.

[6] M. M. El Missiry, "Excitation control of a brushless synchronous motor," *IEEE Trans. Ind. Appl.*, vol. IA-20, no. 5, pp. 1285–1289, Sep. 1984.

[7] A. Tessarolo, G. Zocco, and C. Tonello, "Design and testing of a 45-MW 100-Hz quadruple-star synchronous motor for a liquefied natural gas turbo-compressor drive," *IEEE Trans. Ind. Appl.*, vol. 47, no. 3, pp. 1210–1219, May/Jun. 2011.

[8] S. Schroder, P. Tenca, T. Geyer, P. Soldi, L. Garces, R. Zhang, T. Toma, and P. Bordignon, "Modular high-power shunt-interleaved drive system: A realization up to 35 MW for oil & gas applications," *IEEE Trans. Ind. Appl.*, vol. 46, no. 2, pp. 821–830, Mar./Apr. 2010.

[9] M. Olivo, N. Barbini, A. Tessarolo, S. Cicutto, and G. Zocco, "Start-up performance prediction of line-fed solid-rotor salient-pole synchronous motors," in *Proc. 13th Int. Conf. Elect. Mach.*, Sep. 2018, pp. 407–413.

[10] J. L. Kirtley, A. Banerjee, and S. Englebretson, "Motors for ship propulsion," *Proc. IEEE*, vol. 103, no. 12, pp. 2320–2332, Dec. 2015.

[11] S. Nuzzo, M. Galea, P. Bolognesi, G. Vakil, D. Fallows, C. Gerada, and N. Brown, "A methodology to remove stator skew in small–medium size synchronous generators via innovative damper cage designs," *IEEE Trans. Ind. Electron.*, vol. 66, no. 6, pp. 4296–4307, Jun. 2019.

[12] S. Nuzzo, P. Bolognesi, C. Gerada, and M. Galea, "Simplified damper cage circuital model and fast analytical–numerical approach for the analysis of synchronous generators," *IEEE Trans. Ind. Electron.*, vol. 66, no. 11, pp. 8361–8371, Nov. 2019.

[13] Y. Zhang and A. M. Cramer, "Unified model formulations for synchronous machine model with saturation and arbitrary rotor network representation," *IEEE Trans. Energy Convers.*, vol. 31, no. 4, pp. 1356–1365, Dec. 2016.

[14] J. K. Nøland, M. Giset, and E. F. Alves, "Continuous evolution and modern approaches of excitation systems for synchronous machines," in *Proc. 13th Int. Conf. Elect. Mach.*, Sep. 2018, pp. 104–110.

[15] X. Sun, C. Hu, J. Zhu, S. Wang, W. Zhou, Z. Yang, G. Lei, K. Li, B. Zhu, and Y. Guo, "MPTC for PMSMs of EVs with multi-motor driven system considering optimal energy allocation," *IEEE Trans. Magn.*, vol. 55, no. 7, Jul. 2019, Art. no. 8104306.

[16] X. Sun, C. Hu, G. Lei, Y. Guo, and J. Zhu, "State feedback control for a PM hub motor based on grey wolf optimization algorithm," *IEEE Trans. Power Electron.*, to be published.

[17] *Report on Coordination of Grid Codes and Generator Standards: Consequences of Diverse Grid Code Requirements on Synchronous Machine Design and Standards*, document PES-TR69, Feb. 2019, pp. 1–88.

[18] D. S. Karl and R. C. Schaefer, "NERC power industry policies," *IEEE Ind. Appl. Mag.*, vol. 10, no. 2, pp. 30–38, Mar. 2004.

[19] F. Yao, Q. An, X. Gao, L. Sun, and T. A. Lipo, "Principle of operation and performance of a synchronous machine employing a new harmonic excitation scheme," *IEEE Trans. Ind. Appl.*, vol. 51, no. 5, pp. 3890–3898, Sep./Oct. 2015.

[20] F. Yao, Q. An, L. Sun, and T. A. Lipo, "Performance investigation of a brushless synchronous machine with additional harmonic field windings," *IEEE Trans. Ind. Electron.*, vol. 63, no. 11, pp. 6756–6766, Nov. 2016.

[21] Y. T. Rao, C. Chakraborty, and S. Basak, "Brushless induction excited synchronous generator with induction machine operating in plugging mode," *IEEE Trans. Ind. Appl.*, vol. 54, no. 6, pp. 5748–5759, Nov./Dec. 2018.

[22] C. Chakraborty and Y. T. Rao, "Performance of brushless induction excited synchronous generator," *IEEE J. Emerg. Sel. Topics Power Electron.*, to be published.

[23] J. Sottile, F. C. Trutt, and A. W. Leedy, "Condition monitoring of brushless three-phase synchronous generators with stator winding or rotor circuit deterioration," *IEEE Trans. Ind. Appl.*, vol. 42, no. 5, pp. 1209–1215, Sep. 2006.

[24] Y. Wu, B. Cai, and Q. Ma, "An online diagnostic method for rotary diode open-circuit faults in brushless exciters," *IEEE Trans. Energy Convers.*, vol. 33, no. 4, pp. 1677–1685, Dec. 2018.

[25] W. Yucai, C. Bochong, and M. Qianqian, "Research on an online diagnosis for rotating diode faults in three-phase brushless exciter with two coils," *IET Electr. Power Appl.*, vol. 13, no. 1, pp. 101–109, 2019.

[26] I. C. Report, "Excitation system models for power system stability studies," *IEEE Trans. Power App. Syst.*, vol. PAS-100, no. 2, pp. 494–509, Feb. 1981.

[27] D. R. Fenwick and W. F. Wright, "Review of trends in excitation systems and possible future developments," *Proc. Inst. Elect. Eng.*, vol. 123, no. 5, pp. 413–420, May 1976.

[28] W. F. Wright, R. Hawley, and J. L. Dinely, "Brushless thyristor excitation systems," *IEEE Trans. Power App. Syst.*, vol. PAS-91, no. 5, pp. 1848–1854, Sep. 1972.

[29] A. Godhwani, M. J. Basler, K. Kim, and T. W. Eberly, "Commissioning experience with a modern digital excitation system," *IEEE Trans. Energy Convers.*, vol. 13, no. 2, pp. 183–187, Jun. 1998.

[30] R. C. Schaefer and K. Kim, "Excitation control of the synchronous generator," *IEEE Ind. Appl. Mag.*, vol. 7, no. 2, pp. 37–43, Mar. 2001.

[31] K. Kim and R. C. Schaefer, "Tuning a PID controller for a digital excitation control system," *IEEE Trans. Ind. Appl.*, vol. 41, no. 2, pp. 485–492, Mar. 2005.

[32] C. Schaefer, "Digital excitation systems—Growing obsolescence of aging systems," in *Proc. Annu. Pulp, Paper Forest Ind. Tech. Conf. (PPFIC)*, Jun. 2017, pp. 1–7.

[33] D. X. Llano, S. Abdi, M. Tatlow, E. Abdi, and R. A. McMahon, "Energy harvesting and wireless data transmission system for rotor instrumentation in electrical machines," *IET Power Electron.*, vol. 10, no. 11, pp. 1259–1267, Sep. 2017.

[34] E. Silander, "Rotating electrical machine," U.S. Patent 9 325 225, Apr. 26, 2016.

[35] Voith. (Apr. 2013). *Maintenance Free Exciter*. [Online]. Available: http://voith.com/br/t3383_Maintenance_Free_Exciter_screen.pdf

[36] J. K. Nøland, F. Evestedt, J. J. Pérez-Loya, J. Abrahamsson, and U. Lundin, "Testing of active rectification topologies on a six-phase rotating brushless outer pole PM exciter," *IEEE Trans. Energy Convers.*, vol. 33, no. 1, pp. 59–67, Mar. 2018.

[37] J. K. Nøland, F. Evestedt, J. J. Pérez-Loya, J. Abrahamsson, and U. Lundin, "Design and characterization of a rotating brushless outer pole PM exciter for a synchronous generator," *IEEE Trans. Ind. Appl.*, vol. 53, no. 3, pp. 2016–2017, May/Jun. 2017.

[38] J. K. Nøland, F. Evestedt, J. J. Pérez-Loya, J. Abrahamsson, and U. Lundin, "Comparison of thyristor rectifier configurations for a six-phase rotating brushless outer pole PM exciter," *IEEE Trans. Ind. Electron.*, vol. 65, no. 2, pp. 968–976, Feb. 2018.

[39] E. Jung, S. Kim, J.-I. Ha, and S.-K. Sul, "Control of a synchronous motor with an inverter integrated rotor," *IEEE Trans. Ind. Appl.*, vol. 48, no. 6, pp. 1993–2001, Nov./Dec. 2012.

[40] S. Choe, E. Jung, and S.-K. Sul, "Sensorless control of synchronous machine with an inverter integrated rotor," *IEEE Trans. Ind. Appl.*, vol. 50, no. 4, pp. 2584–2591, Jul. 2014.

[41] D.-H. Lee, "Design and direct field current control scheme of a synchronous generator with PM exciter based on the reference frequency," *IET Electr. Power Appl.*, vol. 13, no. 8, pp. 1150–1156, 2019.

[42] M. S. Griffith, "Modem AC generator control systems: Some plain and painless facts," *IEEE Trans. Ind. Appl.*, vol. IA-14, no. 6, pp. 481–491, Nov. 1978.

[43] *IEEE Guide for Identification, Testing, and Evaluation of the Dynamic Performance of Excitation Control Systems*, IEEE Standard 421.2-2014, Jun. 2014, pp. 1–63.

[44] *IEEE Guide for the Preparation of Excitation System Specifications*, IEEE Standard 421.4-2014, Apr. 2014, pp. 1–57.

[45] A.-J. Nikkila, A. Kuusela, M. Laasonen, L. Haarla, and A. Pahkin, "Self-excitation of a synchronous generator during power system restoration," *IEEE Trans. Power Syst.*, to be published.

[46] R. C. Schaefer, "Specifying excitation systems for procurement," in *Proc. Annu. Pulp Paper Ind. Tech. Conf. (PPFIC)*, Jun. 2010, pp. 1–11.

[47] R. Schaefer, D. Jansen, S. McMullen, and P. Rao, "Coordination of digital excitation system settings for reliable operation," in *Proc. Annu. Pulp Paper Ind. Tech. Conf. (PPFIC)*, Jun. 2011, pp. 112–119.

[48] S. Khan, "Application aspects of generator and excitation system for process plants," *IEEE Trans. Ind. Appl.*, vol. 35, no. 3, pp. 703–712, May 1999.

[49] G. Klempner and I. Kerszenbaum. (2018). *Principles Operation Synchronous Machines*. [Online]. Available: https://ieeexplore.ieee.org/document/8410159

[50] E. Rebollo, F. R. Blanquez, C. A. Platero, F. Blazquez, and M. Redondo, "Improved high-speed de-excitation system for brushless synchronous machines tested on a 20 MVA hydro-generator," *IET Electr. Power Appl.*, vol. 9, no. 6, pp. 405–411, Jul. 2015.

[51] R. Thornton-Jones, I. Golightly, N. Gutteridge, C. Huizer, and D. Navratil, "Review of generator and excitation system specification and test requirements to satisfy multiple international grid code standards," in *Proc. IEEE Power Energy Soc. Gen. Meeting*, Jul. 2012, pp. 1–6.

[52] D. dos Santos Mota and C. Goldemberg, "Comparison between voltage control structures of synchronous machines," *IEEE Latin Amer. Trans.*, vol. 8, no. 6, pp. 631–636, Dec. 2010.

[53] K. Kim, P. Rao, and J. A. Burnworth, "Self-tuning of the PID controller for a digital excitation control system," *IEEE Trans. Ind. Appl.*, vol. 46, no. 4, pp. 1518–1524, Jul./Aug. 2010.

[54] Y.-Y. Hsu, C.-S. Liu, T.-S. Luor, C.-L. Chang, A.-S. Liu, Y.-T. Chen, and C.-T. Huang, "Experience with the identification and tuning of excitation system parameters at the second nuclear power plant of Taiwan power company," *IEEE Trans. Power Syst.*, vol. 11, no. 2, pp. 747–753, May 1996.

[55] D. dos Santos Mota, "Estimating the frequency response of an excitation system and synchronous generator: Sinusoidal disturbances versus empirical transfer function estimate," *IEEE Power Energy Technol. Syst. J.*, vol. 5, no. 2, pp. 27–34, Jun. 2018.

[56] *IEEE Recommended Practice for the Specification and Design of Field Discharge Equipment for Synchronous Machines*, IEEE Standard 421.6-2017, Jun. 2017, pp. 1–38.

[57] J. Taborda, "Modern technical aspects of field discharge equipment for excitation systems," in *Proc. IEEE Power Energy Soc. Gen. Meeting-Convers. Del. Elect. Energy 21st Century*, Jul. 2008, pp. 1–8.

[58] R. Mutukutti, D. Apps, and C. Henville, "Field breaker tripping options for generator static excitation systems with ac field circuit breakers—A case study," in *Proc. IEEE PES Gen. Meeting*, Jul. 2010, pp. 1–6.

[59] T. L. Dillman, F. W. Keay, C. Raczkowski, J. W. Skooglund, and W. H. South, "Brushless excitation," *IEEE Spectr.*, vol. 9, no. 3, pp. 58–66, Mar. 1972.

[60] I. A. Gibbs and D. S. Kimmel, "Active current balance between parallel thyristors in multi-bridge AC-DC rectifiers," *IEEE Trans. Energy Convers.*, vol. 16, no. 4, pp. 334–339, Dec. 2001.

[61] I. A. Gibbs, "Testing of active current balance in parallel thyristor bridges," *IEEE Trans. Energy Convers.*, vol. 20, no. 2, pp. 481–484, Jun. 2005.

[62] I. A. Gibbs, "Control system and method employing active temperature balance for controlling rectifier bridge," U.S. Patent 6 724 643 B1, Apr. 20, 2004.

[63] I. A. Gibbs, "Controlled rectifier bridge, control system, and method for controlling rectifier bridge by disabling gate control signals," U.S. Patent 6 998 735 B2, Feb. 14, 2006.

[64] I. A. Gibbs, "Method and control system employing conduction monitors for detecting unbalanced current condition of alternating current phases," U.S. Patent 7 012 823 B2, Mar. 14, 2006.

[65] R. S. Jordan, R. C. Schaefer, J. A. Estes, and M. R. Dube, "Good as new," *IEEE Ind. Appl. Mag.*, vol. 11, no. 2, pp. 31–38, Mar. 2005.

[66] R. C. Schaefer, "Applying static excitation systems," *IEEE Ind. Appl. Mag.*, vol. 4, no. 6, pp. 41–49, Nov. 1998.

[67] J. P. Bayne, P. Kundur, and W. Watson, "Static exciter control to improve transient stability," *IEEE Trans. Power App. Syst.*, vol. PAS-94, no. 4, pp. 1141–1146, Jul. 1975.

[68] S.-H. Park, S.-K. Lee, S.-W. Lee, J.-S. Yu, S.-S. Lee, and C.-Y. Won, "Output voltage control of a synchronous generator for ships using compound type digital AVR," in *Proc. 31st Int. Telecommun. Energy Conf. (INTELEC)*, Oct. 2009, pp. 1–6.

[69] K. Kamiev, J. Nerg, J. Pyrhonen, V. Zaboin, and J. Tapia, "Feasibility of an armature-reaction-compensated permanent-magnet synchronous generator in island operation," *IEEE Trans. Ind. Electron.*, vol. 61, no. 9, pp. 5075–5085, Sep. 2014.

[70] L. Díez-Maroto, L. Rouco, and F. Fernández-Bernal, "Modeling, sizing, and control of an excitation booster for enhancement of synchronous generators fault ride-through capability: Experimental validation," *IEEE Trans. Energy Convers.*, vol. 31, no. 4, pp. 1304–1314, Dec. 2016.

[71] R. Joho, "Static exciter system for a generator and method of operation," U.S. Patent 8 008 895 B2, Aug. 30, 2011.

[72] L. Díez-Maroto, J. Renedo, L. Rouco, and F. Fernández-Bernal, "Lyapunov stability based wide area control systems for excitation boosters in synchronous generators," *IEEE Trans. Power Syst.*, vol. 34, no. 1, pp. 194–204, Jan. 2019.

[73] Z. Chen, C. Mao, D. Wang, J. Lu, and Y. Zhou, "Design and implementation of voltage source converter excitation system to improve power system stability," *IEEE Trans. Ind. Appl.*, vol. 52, no. 4, pp. 2778–2788, Jul./Aug. 2016.

[74] C. W. Taylor, J. R. Mechenbier, and C. E. Matthews, "Transient excitation boosting at Grand Coulee Third Power plant: Power system application and field tests," *IEEE Trans. Power Syst.*, vol. 8, no. 3, pp. 1291–1298, Aug. 1993.

[75] H.-W. Rhew, S.-K. Sul, and M.-H. Park, "A new generator static excitation system using boost-buck chopper," in *Proc. 22nd Annu. Conf. IEEE Ind. Electron. Soc.*, vol. 2, Aug. 1996, pp. 1023–1028.

[76] J. R. Rodriguez, J. Pontt, C. Silva, E. P. Wiechmann, P. W. Hammond, F. W. Santucci, R. Alvarez, R. Musalem, S. Kouro, and P. Lezana, "Large current rectifiers: State of the art and future trends," *IEEE Trans. Ind. Electron.*, vol. 52, no. 3, pp. 738–746, Jun. 2005.

[77] A. Siebert, A. Troedson, and S. Ebner, "AC to DC power conversion now and in the future," *IEEE Trans. Ind. Appl.*, vol. 38, no. 4, pp. 934–940, Jul./Aug. 2002.

[78] T. L. Dillman, J. W. Skooglund, F. W. Keay, W. H. South, and C. Raczkowski, "A high initial response brushless excitation system," *IEEE Trans. Power App. Syst.*, vol. PAS-90, no. 5, pp. 2089–2094, Sep. 1971.

[79] J. D. Hurley and M. S. Baldwin, "High-Response Excitation Systems on Turbine-Generators: A Stability Assessment," *IEEE Trans. Power App. Syst.*, vol. PAS-101, no. 11, pp. 4211–4221, Nov. 1982.

[80] C. A. Stigers, J. D. Hurley, D. I. Gorden, and D. M. Callanan, "Field tests and simulation of a high initial response brushless excitation system," *IEEE Trans. Energy Convers.*, vol. EC-1, no. 1, pp. 2–10, Mar. 1986.

[81] Stamford, CT, USA. *Alternator Applications*. 2018. [Online]. Available: https://stamford-avk.com/cummins-alternator-applications

[82] G. Laliberte, "A comparison of generator excitation systems (power topic 6008—Technical information from cummins power generation)," Cummins Power Gener., Peterborough, U.K., Tech. Rep. GLPT-6008-EN (10/14), Oct. 2014, pp. 1–6.

[83] L. Somer. (2013). *Low Voltage Alternators–Excitation and Regulation Systems*. [Online]. Available: http://www.leroy-somer.com/documentation_pdf/4124a_en.pdf

[84] S. Nuzzo, M. Galea, C. Gerada, and N. Brown, "Analysis, modeling, and design considerations for the excitation systems of synchronous generators," *IEEE Trans. Ind. Electron.*, vol. 65, no. 4, pp. 2996–3007, Apr. 2018.

[85] N. Jakeman, M. J. Wright, D. H. Dalby, and N. Brown, "Method and apparatus for controlling excitation," U.S. Patent 7 843 175 B2, Nov. 30, 2010.

[86] M. Tartibi and A. Domijan, "Optimizing AC-exciter design," *IEEE Trans. Energy Convers.*, vol. 11, no. 1, pp. 16–24, Mar. 1996.
[87] C. M. Hansen, Jr., and A. W. Wohlberg, "Combination exciter/permanent magnet generator for brushless generator system," U.S. Patent 4 223 263 A, Sep. 16, 1980.
[88] T. D. Fluegel, "Generator system with integral permanent magnet generator exciter," U.S. Patent 4 755 736 A, Jul. 5, 1988.
[89] S.-H. Park, J.-S. Yu, S.-S. Lee, S.-W. Lee, and C.-Y. Won, "Output voltage control of synchronous generator for ships using a PMG type digital AVR," in *Proc. IEEE Energy Convers. Congr. Expo.*, Sep. 2009, pp. 417–421.
[90] O. Wasynczuk, L. J. Rashkin, S. D. Pekarek, R. R. Swanson, B. P. Loop, N. Wu, S. F. Glover, and J. C. Neely, "Voltage and frequency regulation strategies in isolated AC micro-grids," in *Proc. Int. Conf. Cyber Technol. Automat., Control, Intell. Syst. (CYBER)*, May 2012, pp. 5–10.
[91] H. Gorginpour, "Optimal design of brushless AC exciter for large synchronous generators considering grid codes requirements," *IET Gener., Transmiss. Distrib.*, vol. 12, no. 17, pp. 3954–3962, 2018.
[92] V. Madonna, P. Giangrande, and M. Galea, "Electrical power generation in aircraft: Review, challenges, and opportunities," *IEEE Trans. Transport. Electrific.*, vol. 4, no. 3, pp. 646–659, Sep. 2018.
[93] M. Ibrahim and P. Pillay, "Hysteresis-dependent model for the brushless exciter of synchronous generators," *IEEE Trans. Energy Convers.*, vol. 30, no. 4, pp. 1321–1328, Dec. 2015.
[94] A. Barakat, S. Tnani, G. Champenois, and E. Mouni, "Monovariable and multivariable voltage regulator design for a synchronous generator modeled with fixed and variable loads," *IEEE Trans. Energy Convers.*, vol. 26, no. 3, pp. 811–821, Sep. 2011.
[95] M. Gunes and N. Dogru, "Fuzzy control of brushless excitation system for steam turbogenerators," *IEEE Trans. Energy Convers.*, vol. 25, no. 3, pp. 844–852, Sep. 2010.
[96] H. K. Bui, N. Bracikowski, M. Hecquet, K.-L. Zappellini, and J.-P. Ducreux, "Simulation of a large power brushless synchronous generator (BLSG) with a rotating rectifier by a reluctance network for fault analysis and diagnosis," *IEEE Trans. Ind. Appl.*, vol. 53, no. 5, pp. 4327–4337, Oct. 2017.
[97] G. W. McLean, "Auxiliary winding for a generator," U.S. Patent 9 882 518 B2, Jan. 30, 2018.
[98] X. Sun, Z. Shi, L. Chen, and Z. Yang, "Internal model control for a bearingless permanent magnet synchronous motor based on inverse system method," *IEEE Trans. Energy Convers.*, vol. 31, no. 4, pp. 1539–1548, Dec. 2016.
[99] X. Sun, L. Chen, H. Jiang, Z. Yang, J. Chen, and W. Zhang, "High-performance control for a bearingless permanent-magnet synchronous motor using neural network inverse scheme plus internal model controllers," *IEEE Trans. Ind. Electron.*, vol. 63, no. 6, pp. 3479–3488, Jun. 2016.
[100] P. C. Kjaer, T. Kjellqvist, and C. Delaloye, "Estimation of field current in vector-controlled synchronous machine variable-speed drives employing brushless asynchronous exciters," *IEEE Trans. Ind. Appl.*, vol. 41, no. 3, pp. 834–840, May 2005.
[101] Z. Zhang, W. Liu, J. Peng, D. Zhao, T. Meng, J. Pang, and C. Sun, "Identification of TBAES rotating diode failure," *IET Elect. Power Appl.*, vol. 11, no. 2, pp. 260–271, Feb. 2017.
[102] Z. Zhang, W. Liu, D. Zhao, S. Mao, T. Meng, and N. Jiao, "Steady-state performance evaluations of three-phase brushless asynchronous excitation system for aircraft starter/generator," *IET Elect. Power Appl.*, vol. 10, no. 8, pp. 788–798, Sep. 2016.
[103] V. Ruuskanen, M. Niemelä, J. Pyrhönen, S. Kanerva, and J. Kaukonen, "Modelling the brushless excitation system for a synchronous machine," *IET Elect. Power Appl.*, vol. 3, no. 3, pp. 231–239, May 2009.
[104] N. Jiao, W. Liu, Z. Zhang, T. Meng, J. Peng, and Y. Jiang, "Field current estimation for wound-rotor synchronous starter–generator with asynchronous brushless exciters," *IEEE Trans. Energy Convers.*, vol. 32, no. 4, pp. 1554–1561, Dec. 2017.
[105] N. Jiao, W. Liu, T. Meng, C. Sun, and Y. Jiang, "Decoupling control for aircraft brushless wound-rotor synchronous starter-generator in the starting mode," *J. Eng.*, vol. 2018, no. 13, pp. 581–586, 2018.
[106] S. Mao, W. Liu, N. Jiao, G. Luo, Y. Jiang, and Y. Hu, "Design and implementation of parameter estimation and start control of brushless synchronous starter/generators under sudden excitation change," *IEEE Trans. Ind. Electron.*, to be published.
[107] J. Wei, H. Xu, B. Zhou, Z. Zhang, and C. Gerada, "An integrated method for three-phase AC excitation and high-frequency voltage signal injection for sensorless starting of aircraft starter/generator," *IEEE Trans. Ind. Electron.*, vol. 66, no. 7, pp. 5611–5622, Jul. 2019.
[108] S. Mao, W. Liu, Z. Chen, N. Jiao, and J. Peng, "Rotor position estimation of brushless synchronous starter/generators by using the main exciter as a position sensor," *IEEE Trans. Power Electron.*, to be published.
[109] N. Jiao, W. Liu, T. Meng, J. Peng, and S. Mao, "Design and control of a two-phase brushless exciter for aircraft wound-rotor synchronous starter/generator in the starting mode," *IEEE Trans. Power Electron.*, vol. 31, no. 6, pp. 4452–4461, Jun. 2016.
[110] A. Griffo, R. Wrobel, P. H. Mellor, and J. M. Yon, "Design and characterization of a three-phase brushless exciter for aircraft starter/generator," *IEEE Trans. Ind. Appl.*, vol. 49, no. 5, pp. 2106–2115, Oct. 2013.
[111] J. Tang and Y. Liu, "Design and experimental verification of a 48 V 20 kW electrically excited synchronous machine for mild hybrid vehicles," in *Proc. 13th Int. Conf. Elect. Mach. (ICEM)*, Sep. 2018, pp. 649–655.
[112] C. Stancu, T. Ward, K. Rahman, R. Dawsey, and P. Savagian, "Separately excited synchronous motor with rotary transformer for hybrid vehicle application," *IEEE Trans. Ind. Appl.*, vol. 54, no. 1, pp. 223–232, Jan. 2018.
[113] M. Tosi, "Rotary transformer design for brushless electrically excited synchronous machines," M.S. thesis, Laurea Magistrale Ingegneria Elettrica, Universita Degli Studi Padova, 2014.
[114] R. Trevisan and A. Costanzo, "A 1-kW contactless energy transfer system based on a rotary transformer for sealing rollers," *IEEE Trans. Ind. Electron.*, vol. 61, no. 11, pp. 6337–6345, Nov. 2014.
[115] S.-A. Vip, J.-N. Weber, A. Rehfeldt, and B. Ponick, "Rotary transformer with ferrite core for brushless excitation of synchronous machines," in *Proc. 22nd Int. Conf. Elect. Mach. (ICEM)*, Sep. 2016, pp. 890–896.
[116] Y. Liu, D. Pehrman, O. Lykartsis, J. Tang, and T. Liu, "High frequency exciter of electrically excited synchronous motors for vehicle applications," in *Proc. 22nd Int. Conf. Elect. Mach. (ICEM)*, Sep. 2016, pp. 378–383.
[117] J. Tang, Y. Liu, and N. Sharma, "Modeling and experimental verification of high-frequency inductive brushless exciter for electrically excited synchronous machines," *IEEE Trans. Ind. Appl.*, to be published.
[118] E. Rebollo, C. A. Platero, F. Blazquez, and R. Granizo, "Internal sudden short-circuit response of a new HSBDS for brushless synchronous machines tested on a 15 MVA generator," *IET Electr. Power Appl.*, vol. 11, no. 4, pp. 495–503, Apr. 2017.
[119] C. Platero, M. Redondo, F. Blázquez, and P. Frìas, "High-speed de-excitation system for brushless synchronous machines," *IET Electr. Power Appl.*, vol. 6, no. 3, pp. 156–161, 2012.
[120] C. A. P. Gaona, F. B. García, P. F. Marín, M. R. Cuevas, R. G. Arrabé, and C. C. López, "Rapid de-excitation system for synchronous machines with indirect excitation," U.S. Patent 13 201 971, Dec. 8, 2011.
[121] J. K. Nøland, F. Evestedt, J. J. Pérez-Loya, J. Abrahamsson, and U. Lundin, "Design and characterization of a rotating brushless PM exciter for a synchronous generator test setup," in *Proc. 12th Int. Conf. Elect. Mach. (ICEM)*, vol. 1, Sep. 2016, pp. 402–409.
[122] J. K. Nøland, F. Evestedt, and U. Lundin, "Failure modes demonstration and redundant postfault operation of rotating thyristor rectifiers on brushless dual-star exciters," *IEEE Trans. Ind. Electron.*, vol. 66, no. 2, pp. 842–851, Feb. 2019.
[123] J. K. Nøland, F. Evestedt, and U. Lundin, "Active current sharing control method for rotating thyristor rectifiers on brushless dual-star exciters," *IEEE Trans. Energy Convers.*, vol. 33, no. 2, pp. 893–896, Jun. 2018.
[124] J. K. Nøland and U. Lundin, "Step time response evaluation of different synchronous generator excitation systems," in *Proc. IEEE Int. Energy Conf. (ENERGYCON)*, Apr. 2016, pp. 1–7.
[125] D. C. Ludois, J. K. Reed, and K. Hanson, "Capacitive power transfer for rotor field current in synchronous machines," *IEEE Trans. Power Electron.*, vol. 27, no. 11, pp. 4638–4645, Nov. 2012.
[126] J. Dai and D. C. Ludois, "Single active switch power electronics for kilowatt scale capacitive power transfer," *IEEE J. Emerg. Sel. Topics Power Electron.*, vol. 3, no. 1, pp. 315–323, Mar. 2015.
[127] A. Di Gioia, I. P. Brown, Y. Nie, R. Knippel, D. C. Ludois, J. Dai, S. Hagen, and C. Alteheld, "Design and demonstration of a wound field synchronous machine for electric vehicle traction with brushless capacitive field excitation," *IEEE Trans. Ind. Appl.*, vol. 54, no. 2, pp. 1390–1403, Mar./Apr. 2018.

[128] J. K. Nøland, F. Evestedt, J. J. Pérez-Loya, J. Abrahamsson, and U. Lundin, "Evaluation of different power electronic interfaces for control of a rotating brushless PM exciter," in *Proc. 42nd Annu. Conf. IEEE Ind. Electron. Soc.*, Oct. 2016, pp. 1924–1929.
[129] J. K. Nøland, K. B. Hjelmervik, and U. Lundin, "Comparison of thyristor-controlled rectification topologies for a six-phase rotating brushless permanent magnet exciter," *IEEE Trans. Energy Convers.*, vol. 31, no. 1, pp. 314–322, Mar. 2016.
[130] J. K. Nøland, "A new paradigm for large brushless hydrogenerators: Advantages beyond the static system," Ph.D. dissertation, Fac. Sci. Technol., Ångström Lab., Uppsala Univ., Uppsala, Sweden, 2017.
[131] J. Dai, S. Hagen, D. C. Ludois, and I. P. Brown, "Synchronous generator brushless field excitation and voltage regulation via capacitive coupling through journal bearings," *IEEE Trans. Ind. Appl.*, vol. 53, no. 4, pp. 3317–3326, Jul. 2017.
[132] L. R. Roche, "A harmonic excitation system for turbine generators," *Trans. Amer. Inst. Elect. Eng. III, Power App. Syst.*, vol. 81, no. 4, pp. 281–284, Apr. 1962.
[133] G. Shrestha, D. Tremelling, W. Arshad, W. Ouyang, and J. Westerlund, "Systems and methods concerning exciterless synchronous machines," U.S. Patent 14/598 926, Jan. 16, 2015.
[134] G. Jawad, Q. Ali, T. A. Lipo, and B. I. Kwon, "Novel brushless wound rotor synchronous machine with zero-sequence third-harmonic field excitation," *IEEE Trans. Magn.*, vol. 52, no. 7, pp. 1–4, Jul. 2016.
[135] C. Chakraborty, S. Basak, and T. R. Yalla, "Synchronous generator with embedded brushless synchronous exciter," *IEEE Trans. Energy Convers.*, to be published.
[136] S. Nonaka and H. Takami, "Low-speed drive of PWM-VSI-fed brushless self-excited synchronous motor," *IEEE Trans. Ind. Appl.*, vol. IA-22, no. 5, pp. 847–852, Sep. 1986.
[137] F. Shibata and T. Fukami, "A brushless and exciterless polyphase synchronous motor," *IEEE Trans. Energy Convers.*, vol. EC-2, no. 3, pp. 480–488, Sep. 1987.
[138] F. Shibata and T. Fukami, "An exciterless- and brushless-type commutatorless motor fed from a transformer in parallel with a voltage source inverter," *IEEE Trans. Ind. Appl.*, vol. 25, no. 6, pp. 1118–1125, Nov. 1989.
[139] F. Shibata, T. Fukami, and N. Naoe, "A brushless, exciterless, single-phase, sinusoidal wave synchronous machine having an auxiliary stator winding," *IEEE Trans. Energy Convers.*, vol. 4, no. 2, pp. 272–278, Jun. 1989.
[140] S. Nonaka and K. Kesamaru, "Analysis of voltage-adjustable brushless synchronous generator without exciter," *IEEE Trans. Ind. Appl.*, vol. 25, no. 1, pp. 126–132, Jan. 1989.
[141] S. Nonaka and T. Kawaguchi, "Excitation scheme of brushless self-excited-type three-phase synchronous machine," *IEEE Trans. Ind. Appl.*, vol. 28, no. 6, pp. 1322–1329, Nov. 1992.
[142] K. Inoue, H. Yamashita, E. Nakamae, and T. Fujikawa, "A brushless self-exciting three-phase synchronous generator utilizing the 5th-space harmonic component of magneto motive force through armature currents," *IEEE Trans. Energy Convers.*, vol. 7, no. 3, pp. 517–524, Sep. 1992.
[143] S. Nonaka and T. Kawaguchi, "A new variable-speed AC generator system using a brushless self-excited-type synchronous machine," *IEEE Trans. Ind. Appl.*, vol. 28, no. 2, pp. 490–496, Mar. 1992.
[144] S. Nonaka, K. Kesamaru, and K. Horita, "Analysis of brushless four-pole three-phase synchronous generator without exciter by the finite element method," *IEEE Trans. Ind. Appl.*, vol. 30, no. 3, pp. 615–620, May 1994.
[145] S. Satake, K. Inoue, Y. Onogi, H. Yamashita, and Y. Hosaka, "Three-phase brushless self-excited synchronous generator with no rotor excitation windings," U.S. Patent 5/694 027, Dec. 2, 1997.
[146] M. Ayub, A. Hussain, G. Jawad, and B.-I. Kwon, "Brushless operation of a wound-field synchronous machine using a novel winding scheme," *IEEE Trans. Magn.*, vol. 55, no. 6, Jun. 2019, Art. no. 8201104.
[147] M. Ayub, S. Atiq, G. J. Sirewal, and B. Kwon, "Fault-tolerant operation of wound field synchronous machine using coil switching," *IEEE Access*, vol. 7, pp. 67130–67138, 2019.
[148] H. Lomei, K. M. Muttaqi, and D. Sutanto, "A new method to determine the activation time of the overexcitation limiter based on available generator rotor thermal capacity for improving long-term voltage instability," *IEEE Trans. Power Syst.*, vol. 32, no. 3, pp. 1711–1720, Aug. 2017.
[149] T. Øyvang, J. K. Nøland, G. J. Hegglid, and B. Lie, "Online model-based thermal prediction for flexible control of an air-cooled hydrogenerator," *IEEE Trans. Ind. Electron.*, vol. 66, no. 8, pp. 6311–6320, Aug. 2019.
[150] U. Lundin, J. J. Pérez-loya, and J. Abrahamsson, "Arrangement and method for force compensation in electrical machines," U.S. Patent 15/527 240, Nov. 23, 2017.
[151] J. J. Pérez-Loya, C. J. D. Abrahamsson, and U. Lundin, "Electromagnetic losses in synchronous machines during active compensation of unbalanced magnetic pull," *IEEE Trans. Ind. Electron.*, vol. 66, no. 1, pp. 124–131, Jan. 2019.
[152] F. Evestedt, "Improving the functionality of synchronous machines using power electronics," Ph.D. dissertation, Division Electr., Angstrom Lab., Uppsala University, Uppsala, Sweden, 2017.
[153] D. Fallows, S. Nuzzo, A. Costabeber, and M. Galea, "Power quality improvement by pre-computed modulated field current for synchronous generators," in *Proc. IEEE Workshop Elect. Mach. Design, Control Diagnosis (WEMDCD)*, Apr. 2017, pp. 127–131.
[154] J. J. Pérez-Loya, C. J. D. Abrahamsson, F. Evestedt, and U. Lundin, "Demonstration of synchronous motor start by rotor polarity inversion," *IEEE Trans. Ind. Electron.*, vol. 65, no. 10, pp. 8271–8273, Oct. 2018.

JONAS KRISTIANSEN NØLAND (S'14–M'17) received the M.Sc. degree in electric power engineering from the Chalmers University of Technology, Gothenburg, Sweden, in 2013, and the Ph.D. degree in engineering physics from Uppsala University, Uppsala, Sweden, in 2017.

In 2017, he became an Associate Professor with the University of South-Eastern Norway (USN). Since December 2018, he has been an Associate Professor with the Department of Electric Power Engineering, Norwegian University of Science and Technology (NTNU). He has been actively involved in the grid standardization of new excitation system technologies for the Scandinavian power system. His current research interests include smart excitation systems and their interplay with the power system, the optimal utilization of electrical machines, and starter-generators for aircraft applications.

Dr. Nøland is a Board Member of the Norwegian Academic Committee of Publication in Technology in Electrical Power Engineering. He is on the Steering Committee of the IEEE Power and Energy Chapter of Norway. He is also a member of the IEEE Industrial Electronics Society (IES), the IES Electric Machines Technical Committee, the IEEE Industry Applications Society (IAS), and the IEEE Power and Energy Society (PES). He regularly serves the scientific community as a Reviewer for several journals and conferences.

STEFANO NUZZO (M'18) received the B.Sc. and M.Sc. degrees in electrical engineering from the University of Pisa, Pisa, Italy, in 2011 and 2014, respectively, and the Ph.D. degree in electrical engineering from the University of Nottingham, Nottingham, U.K., in 2018, where he is currently a Research Fellow of the Power Electronics, Machines and Control (PEMC) Group.

Since January 2019, he has been a Research Fellow of the Department of Engineering Enzo Ferrari, University of Modena and Reggio Emilia, Modena, Italy. His research interests include the analysis, modeling, and optimizations of electrical machines, with a focus on salient-pole synchronous generators and brushless excitation systems for industrial power generation applications. He is also involved in a number of diverse projects related to more electric aircraft initiative and associated fields.

Dr. Nuzzo is a member of the IEEE Industrial Electronics Society (IES) and the IEEE Industry Applications Society (IAS). He regularly serves the scientific community as a Reviewer for several journals and conferences.

ALBERTO TESSAROLO (SM'06) received the Laurea degree in electrical engineering from the University of Padua and the Ph.D. degree in electrical engineering from the University of Trieste, Italy, in 2000 and 2011, respectively.

Before joining the University, he was involved in the design and development of large innovative motors, generators, and drives. Since 2006, he has been with the Engineering and Architecture Department, University of Trieste, Italy, where he teaches the courses in electric machine fundamentals and electric machine design. He leads several funded research projects in cooperation with industrial companies for the study and development of innovative electric motors, generators, and drives. He has authored over 150 international papers in the areas of electrical machines and drives. He has been an Associate Editor of the IEEE TRANSACTIONS ON ENERGY CONVERSION, the IEEE TRANSACTIONS ON INDUSTRY APPLICATIONS, and *IET Electric Power Applications*. He currently serves as the Editor-in-Chief for the IEEE TRANSACTIONS ON ENERGY CONVERSION. He is a member of the Rotating Machinery Technical Committee TC2 (rotating electric machinery) of the International Electrotechnical Commission (IEC). He is also a member of the IEEE Power and Energy Society Electric Machinery Committee, the IEEE Industry Applications Society Electric Machines Committee, and the IEEE Industrial Electronics Society Electric Machines Technical Committee.

ERICK FERNANDO ALVES (S'06–M'08–SM'19) received the Engineering degree in energy and automation from the University of Sao Paulo, Brazil, in 2007, and the M.Sc. degree in electrical engineering from the Arctic University of Norway, Narvik, in 2018. He is currently pursuing the Ph.D. degree with the Department of Electric Power Engineering, Norwegian University of Science and Technology, Trondheim, Norway, with a focus on virtual synchronous machine technologies. He is currently pursuing the Ph.D. degree with the Department of Electric Power Engineering, Norwegian University of Science and Technology, Trondheim, Norway, where he focuses on virtual synchronous machine technologies.

From 2007 to 2018, he held several positions at the Voith Group in Brazil, Norway, and Germany. During this period, he was involved in the design, engineering, commissioning, and development of excitation systems for over 40 power plants in 18 countries. His latest assignment was with Voith Digital Ventures, Heidenheim, Germany, as the Product Manager, where he was responsible for power generation controls, in particular excitation systems and turbine governors.

Mr. Alves is the Treasurer of the IEEE Power and Energy Chapter of Norway. He is also a member of the IEEE Industrial Electronics Society (IES), the IEEE Industry Applications Society (IAS), the IEEE Power and Energy Society (PES), and the IEEE Control Systems Society (CSS).